69-4046

STOCKTON, Alan Norman, 1942-

BLUE CONDENSATIONS ASSOCIATED WITH GALAXIES.

University of Arizona, Ph.D., 1968
Astronomy

University Microfilms, Inc., Ann Arbor, Michigan

BLUE CONDENSATIONS

ASSOCIATED WITH GALAXIES

by

Alan Norman Stockton

A Dissertation Submitted to the Faculty of the

DEPARTMENT OF ASTRONOMY

In Partial Fulfillment of the Requirements
For the Degree of

DOCTOR OF PHILOSOPHY

In the Graduate College

1 9 6 8

THE UNIVERSITY OF ARIZONA

GRADUATE COLLEGE

I hereby recommend that this dissertation prepared under my direction by Alan Norman Stockton

entitled Blue Condensations Associated With Galaxies

be accepted as fulfilling the dissertation requirement of the degree of Doctor of Philosophy

C. Roger Lynds — Dissertation Director

12 July 1968 — Date

After inspection of the final copy of the dissertation, the following members of the Final Examination Committee concur in its approval and recommend its acceptance:*

R. E. Williams	July 18, 1968
Raymond Weymann	July 18, 1968
Bart J. Bok	August 9, 1968
William Grant Tifft	July 15, 1968

*This approval and acceptance is contingent on the candidate's adequate performance and defense of this dissertation at the final oral examination. The inclusion of this sheet bound into the library copy of the dissertation is evidence of satisfactory performance at the final examination.

STATEMENT BY AUTHOR

This dissertation has been submitted in partial fulfillment of the requirements for an advanced degree at The University of Arizona and is deposited in the University Library to be made available to borrowers under rules of the Library.

Brief quotations from this dissertation are allowable without special permission, provided that accurate acknowledgement of source is made. Requests for permission for extended quotation from or reproduction of this manuscript in whole or in part may be granted by the head of the major department or the Dean of the Graduate College when in his judgment the proposed use of the material is in the interests of scholarship. In all other instances, however, permission must be obtained from the author.

SIGNED: Mary Norman Stockton

ACKNOWLEDGMENTS

The author wishes to acknowledge his gratitude for the direct assistance of several individuals during the course of this investigation:

Mrs. Elizabeth Estrada, who has read the entire manuscript and has suggested many improvements in presentation;

Mr. John Lutnes, Mr. Mark Hanna, and Mr. Glynn Pickens of the Kitt Peak photographic laboratory for their excellent work in preparing the photographic illustrations;

Miss Grace Foley, Mrs. Goldie Ruark, and Mrs. Sylvia Demko for their assistance in locating materials in the Kitt Peak library;

Dr. Bart J. Bok, who served as my faculty advisor during the early stages of the investigation, and whose contagious enthusiasm has been a constant source of encouragement;

Dr. Bengt Westerlund, my current faculty advisor, who has read this dissertation in draft form and has made several valuable suggestions for its improvement;

and, finally, Dr. C. R. Lynds, the director of this dissertation, with whom I have had the pleasure of working for over three years. He has painstakingly reviewed the various drafts and has made a large number of suggestions relating not only to the scientific content but to the achievement of a clearer and more felicitous presentation.

TABLE OF CONTENTS

TABLE OF CONTENTS Continued

LIST OF TABLES

LIST OF ILLUSTRATIONS

ABSTRACT

A number of elliptical and S0 galaxies having nearby blue condensations have been listed by Ambartsumyan and Shachbazyan. Two of these galaxies, NGC 3561 and IC 1182, have visible bridges or jets connecting to the associated blue condensations, and these galaxies have been the ones most intensively studied in the present investigation. Several other systems similar to those listed by Ambartsumyan and Shachbazyan have been found in a search of the National Geographic-Palomar Observatory Sky Survey plates covering some 1300 square degrees.

Spectroscopic observations have been made of some of these blue knots and the galaxies with which they are associated as well as of certain nearby blue galaxies. Estimates of the electron density have been made for several of the objects on the basis of the relative strengths of the [O II] λλ3726, 3729 lines. Densities are typically a few hundred cm^{-3} or lower, similar to those found in diffuse nebulae.

Calibrated spectrophotometric plates have been obtained for three objects: the bright blue condensation near

NGC 3561, the blue galaxy Haro 4, and a bright knot in a spiral arm. The continua and the emission-line spectra of the three objects are quite similar, except that Haro 4 has a slightly higher level of ionization than the others. The spectral-energy distributions for the three objects are approximately proportional to λ^{-4}. The continua apparently cannot be interpreted as synchrotron radiation or as free-bound, free-free, or two-quantum emission from hydrogen. The most likely explanation for the continuum radiation is that it is of stellar origin, in which case almost all of the light must come from O and B stars. The dimensions of the blue condensations near NGC 3561 and IC 1182 are in the range of 2 to 3 kpc, and their absolute magnitudes are -16 to -17.

The linear alignment of the condensations in the NGC 3561 and IC 1182 systems probably sets an upper limit to their ages of a few times 10^8 years. This fact, taken together with the evidence for a large number of young stars, implies that these condensations are recently formed dwarf galaxies.

I

INTRODUCTION

Because elliptical galaxies have simple and symmetric forms, they are attractive test objects for theories of galaxy formation and evolution. They seem long since to have lost their capacity for star formation on any significant scale; for most elliptical galaxies the salient features can be understood in terms of a model possessing no qualitative distinction from that of a scaled-up globular cluster.

Yet certain elliptical galaxies (in gross morphological characteristics indistinguishable from the others) show peculiarities that cannot be explained solely in terms of stars and their motions. In particular, some of them are strong radio sources, and a significant fraction of giant elliptical galaxies in their nuclei show emission lines that indicate velocity dispersions of several hundred km/sec for the gas. The fact that Baade originally classified the stars in elliptical galaxies as pure population II has sometimes been interpreted as meaning that these systems contain

no dust, but it is well known that two of the dwarf elliptical galaxies in the Local Group (NGC 185 and NGC 205) contain small dust patches. Similar patches, even if generally present, would not be detected in giant elliptical galaxies because of the much greater distances of these systems. It is possible, however, that the reddening toward the center observed in some of these galaxies (Tifft 1963, Wood 1966) indicates a moderate general distribution of dust. Certain giant elliptical galaxies associated with radio sources (e.g. NGC 1316, NGC 4374, and NGC 5128) contain visible obscuration, sometimes in large amounts.

Among the more spectacular examples of peculiar elliptical galaxies is M 87, which is identified with the Virgo A radio source. The well-known jet in this object can be traced from the nucleus of the galaxy radially outward for a distance of about 20"; it has 3 prominent condensations near its tip and a few fainter ones closer to the nucleus. The light from the outer condensations is highly polarized (Baade 1956, Hiltner 1959); this fact, along with the complete absence of detectable spectral lines attributable to the jet (Baade and Minkowski 1954; Lynds, private communication), supports the proposal of Shklovskii (1955) that both

the optical and the radio emission result from the synchrotron mechanism. Recently, M 87 has been detected as an X-ray source (Byram, Chubb, and Friedman 1966, Friedman and Byram 1967). The most complete review and discussion of the available observational material on the M 87 jet is that of Felten (1968).

Searches for Blue Knots Associated with Galaxies

No other galaxies with jets like that of M 87 have been found; this fact, however, says little concerning the frequency of such objects. The jet of M 87 itself is not detectable on long-exposure plates because it lies within the overexposed part of the image of the galaxy. For galaxies much farther away (and M 87 is among the closest of the giant elliptical galaxies) the contrast between a similar jet and the galaxy would be even less, because in width the M 87 jet is either unresolved or just barely resolved. Even with a large image scale and optimum exposure, it would be extremely difficult to detect such a jet. Noting these difficulties, Ambartsumyan and Shachbazyan (1957) proposed that perhaps there exist galaxies similar to M 87, but for which a jet projects completely outside of the galaxy. With the assumption that the jets or their individual

condensations are fairly bright, it was reasonable to make a search of the National Geographic Society-Palomar Observatory Sky Survey charts (henceforth called simply the Sky Survey charts) for objects of this type. In conducting this search, Ambartsumyan and Shachbazyan imposed two restrictions on the type of object to be considered. Yellow and red condensations were not included in the search because such objects could not be distinguished from the frequent dwarf satellites of giant galaxies. Furthermore, only blue objects near elliptical and S0 galaxies were considered, because for spiral and irregular galaxies the search would have been confused by bright O-associations. Both of these restrictions were consistent with the initial proposal to search for objects similar to M 87, and neither was intended to be a prejudgment of the actual nature of the condensations.

Table 1 lists data given by Ambartsumyan and Shachbazyan (1957). The estimated photographic apparent magnitudes and color indices (given in the international system) refer to the blue condensations associated with the galaxies. NGC 3561 is an elliptical or S0 galaxy that is part of a complicated system to be described in more detail in

Table 1 Systems Listed by Ambartsumyan and Shachbazyan

System	α 1950	δ	m_{pg}	CI
NGC 3561	$11^h08^m.5$	$+28^o58'$	19.2	$-0^m.5$
IC 1182	16 03.3	+17 43	19.0	-0.2
Anon 1	5 40.3	-26 08	18.5	-0.4
Anon 2	11 08.0	+28 36	18.6	-0.7
Anon 3	11 39.9	+29 31	18.2	-0.5
Anon 4	10 03.8	- 1 19	19.3	0.0

Table 2 Data on NGC 3561 from Zwicky and Humason (1961)

All values have been adjusted to a Hubble constant of 75 km/sec/Mpc. The small letters following the galaxy type refer to the illustration of NGC 3561 in Figure 1.

Galaxy Type	V_r	Major Diameter	M_v
Elliptical (a)	8550 km/sec	10300 pc	$-20^m.9$
Blue Knot (b)	8839	3500	-16.8
Spiral (c)	8803	16700	-20.6

Chapter II. The important feature of this galaxy for present purposes is a jet that resembles that of M 87 and ends in a prominent blue condensation. IC 1182 (erroneously listed as IC 1181 in the original article) also has a long, fairly straight (although discontinuous) feature projecting from its nucleus toward two blue condensations. The magnitude and color index given in Table 1 refer to the inner of the two condensations.

For the remaining four objects there are no associated jet-like features. The three blue condensations near Anon 2 are (in projection) nearly on a straight line, although not on a line passing through the nucleus of the galaxy. There is, of course, a possibility that these last four objects represent an entirely different phenomenon than do NGC 3561 and IC 1182. While it is possible that the blue condensations were once connected to the nucleus of the nearby elliptical galaxy by a luminous bridge, it is also possible (as Ambartsumyan and Shachbazyan point out) that the condensations are small blue galaxies of independent origin or simply background galaxies.

Following this initial paper, other similar systems were listed by the astronomers at Byurakan Astrophysical

Observatory (Ambartsumyan and Shachbazyan 1958, Shachbazyan and Iskudaryan 1959). Ambartsumyan (1961) noted an extremely blue object very close to the galaxy identified with the Hydra A radio source, and Saakyan (1965) found two blue objects near an elliptical galaxy. Many of these later papers deal with blue objects showing stellar images. At high galactic latitudes, and around magnitude 18 or 19, there is considerable risk that many such objects may prove to be white dwarfs, horizontal branch stars, U Geminorum stars, or quasi-stellar objects unless there is some explicit indication that they are physically associated with the galaxies near which they are found.

A rough calculation of the number of white dwarfs between magnitudes 18 and 19 per square degree at high galactic latitudes will serve as an example. Oort (1958) has estimated that white dwarfs account for about $8 \cdot 10^{-3}$ $M\odot/pc^3$ in the region near the sun and that the mean distance from the galactic plane $\bar{z}$ for a white dwarf is 270 pc. If the mean mass for a white dwarf is assumed to be 0.8 $\odot$, the number density of white dwarfs in the galactic plane in the neighborhood of the sun is 10^{-2}. We assume the number

density of white dwarfs at a distance z from the galactic plane to be given by

$$N_{wd}(z) = N_{wd}(0) \exp(-z/\bar{z}).$$

The number of white dwarfs per square degree at the galactic pole having a distance from the galactic plane between z and z + dz is

$$n_{wd}(z)\,dz = N_{wd}(0)\,(\pi/180)^2 z^2 \exp(-z/\bar{z})\,dz.$$

Integrating to find the number of white dwarfs per square degree between z_1 and z_2,

$$n_{wd}(z)\Big|_{z_1}^{z_2} = -N_{wd}(0)\,(\pi/180)^2\,\bar{z} \exp(-z/\bar{z})$$
$$[z^2 + 2z\bar{z} + 2(\bar{z})^2]\Big|_{z_1}^{z_2}.$$

If we may suppose all white dwarfs to have an absolute magnitude of +11.0, then apparent magnitudes of 18 and 19 correspond to distances from the galactic plane of 250 pc and 400 pc, respectively. Therefore, between magnitudes of 18 and 19 the number of white dwarfs per square degree is given by

$$n_{wd}(z)\Big|_{250}^{400} = -(10^{-2})(3.05 \cdot 10^{-4})(270)$$
$$\exp(-z/270)[z^2 + 540z + 14.58 \cdot 10^4]\Big|_{250}^{400} = 14.5.$$

Because $N_{wd}(0)$ and $\bar{z}$ are not accurately known, and because the dispersion in absolute magnitude was ignored, this number is very approximate. It indicates, however, that the probability is about 0.01 that a white dwarf between magnitudes 18 and 19 will be found within 1' of a given galaxy. Several thousand galaxies may be involved in a survey, hence it is likely that some chance coincidences with white dwarfs will be found. More extensive discussions of the frequency and distribution of various kinds of blue stars at high galactic latitudes have been given by Kinman (1965) and by Lynds and Villere (1965).

Previous Spectroscopic Observations

There has been some previous spectroscopic work on NGC 3561 and IC 1182, the two systems mentioned above for which photographic evidence alone seems conclusive in establishing a physical association between the blue knot(s) and the galaxy. A spectrogram of IC 1182 (Burbidge, Burbidge, and Hoyle 1963) failed to record the spectrum of the jet-like feature, but it did reveal a strong emission-line spectrum for the galaxy itself. The tilt of the Hα line indicated a total velocity difference of 350 km/sec for a region 8" long across the nucleus of the galaxy.

Zwicky has published a photograph of NGC 3561 taken with the 200-inch telescope (Zwicky 1956, 1967a) as well as a spectrogram obtained with the slit aligned to pass through the two bright galaxies and the blue knot south of the elliptical galaxy (Zwicky 1958, 1967a). An analysis of this material has been given by Zwicky and Humason (1961); Table 2 gives their principal results. The two galaxies show the H and K lines of Ca II, the G band, and fairly strong [O II] λ3727 emission. The [O II] doublet is also seen in the spectra of the blue knot and the two fainter condensations in the jet. The knot shows a very weak, blue continuum.

The strength of the [O II] λ3727 doublet in the spectra of the three objects is remarkably similar, in spite of the large differences in their continuum strength. This fact points to an important difference between this object and the condensations in the jet of M 87, the spectrum of which shows no lines at all. Whether or not there could be an evolutionary relationship between the two is a matter that will be considered in Chapter IV.

Suggested Origins for Blue Knots and Filamentary Structures

In several survey papers, Ambartsumyan (1958, 1961, 1962, 1965) has expressed the opinion that the blue knots

are dwarf galaxies that have been ejected or split off from the nucleus of the galaxy with which they are associated. This view is consistent with Ambartsumyan's emphasis on the importance of the role of the nucleus in controlling the development and evolution of a galaxy. Zwicky (1967a), discussing NGC 3561 and other systems, states: "...the series of very compact aggregates which are often lined up in a remarkable way point to enormous explosions as the original cause for these formations."

In the past, Zwicky (1956) has explained these and other features in terms of mutual encounters of galaxies and tidal interactions. On the other hand, Ambartsumyan (1958) has argued that long, thin filamentary structures connecting galaxies, if these filaments are composed of stars, cannot in general be due to tidal interactions. This result follows from a consideration of typical relative velocities of such galaxies and an assumption that the velocity dispersion of the stars transverse to the filament is of the order of 30 km/sec or larger.

The remaining interpretation that has been suggested Burbidge et al. 1963) is that these linear features and knots have condensed directly from the intergalactic medium.

These three theories are representative of three general classes into which such theories fall: (a) the observed features (i.e. jets, filaments, blue knots) result from a process intrinsic to the galaxy (although the process may be "triggered" or influenced by objects or events external to the galaxy); (b) they result from an interaction between galaxies; (c) they result from processes occurring external to the galaxy (although their exact form and structure will perhaps be influenced by the galaxy's presence).

General Objectives for the Observations

It has been the purpose of the present study to gather observational material that may be useful in determining the physical nature and the origin of blue knots of the kind found in association with NGC 3561 and IC 1182. The blue knots considered are all fainter than 18th magnitude; there are, therefore, certain restrictions on the type of observations that can reasonably be carried out. An examination of emission-line spectra can yield information concerning excitation and ionization conditions. It is considerably more difficult to study the continua of such faint objects, but, because of the importance of determining the

nature of the continuum radiation, it is worthwhile to try to get some idea of the spectral-energy distribution and to search for absorption lines. From a set of program objects selected on the bases of morphology and color, spectra can provide further evidence relating to the physical homogeneity of the group of objects. Finally, a knowledge of both the spectra and the physical appearances of these blue knots will permit comparisons with more familiar objects.

II

SELECTION OF OBJECTS FOR OBSERVATION

The first list by Ambartsumyan and Shachbazyan (1957) has formed the nucleus of the program objects for the present study. The other lists and identifications mentioned in Chapter I contain no systems of comparable interest to NGC 3561 and IC 1182, nor, in fact, does the survey to be described below. Because of the detail visible in the bridges connecting the galaxies and the blue condensations, these two systems are likely to remain central to any discussion of the problem. Nevertheless, it seemed reasonable to examine the Sky Survey plates in a new search having two major objectives: (a) the discovery of additional systems for which there is evidence of a physical connection between a galaxy and a blue knot, and (b) the discovery of isolated blue galaxies having morphological characteristics similar to those of the blue knots associated with NGC 3561 and IC 1182.

The search was carried out at the Kitt Peak National Observatory with a blink comparator and a set of glass

copies of the Sky Survey plates. An object was considered to be "blue" if its image on the blue-sensitive "O"-plate was substantially larger or denser than its image on the red-sensitive "E"-plate. Approximately 1300 square degrees of the sky were examined, including the entire region from 10^h to 14^h right ascension and from $+27^o$ to $+51^o$ declination. Because the main purpose of the survey was to supply additional objects for spectroscopic investigation, it seemed desirable to cover a large area of the sky rather than to attempt a complete survey of a much smaller region. Accordingly, the resulting list of blue objects near elliptical galaxies (Appendix I) makes no pretense at thoroughness or consistency.

Descriptions of Selected Objects

From the present list, and from published lists, a few of the more interesting systems have been selected to be described here. These are listed in Table 3, and some of them are also illustrated in Figure 1. Numbers preceded by the letter S refer to the list given in Appendix I; those preceded by Arp, VV, and ASh refer, respectively, to the Atlas of Peculiar Galaxies (Arp 1966), the Atlas and Catalogue of Interacting Galaxies (Vorontsov-Velyaminov 1959),

Table 3 Selected Galaxies With Nearby Blue Objects

S Number	Other Designation	α 1950	δ
2		$01^h53^m.5$	$+36^o32'$
--	Hydra A	09 15.7	-11 53
9		10 04.4	+38 07
13		10 22.6	+37 37
17		10 45.0	+39 12
24	ASh 2	11 08.0	+28 36
25	NGC 3561, Arp 105, VV 237	11 08.5	+28 58
26		11 08.9	+03 34
27	ASh 3	11 13.9	+29 31
37		12 43.8	+36 20
41	Arp 196, Herzog 21	13 12.2	+26 24
42		13 12.7	+26 51
48		13 55.1	+29 02
--	IC 1182	16 03.3	+17 56

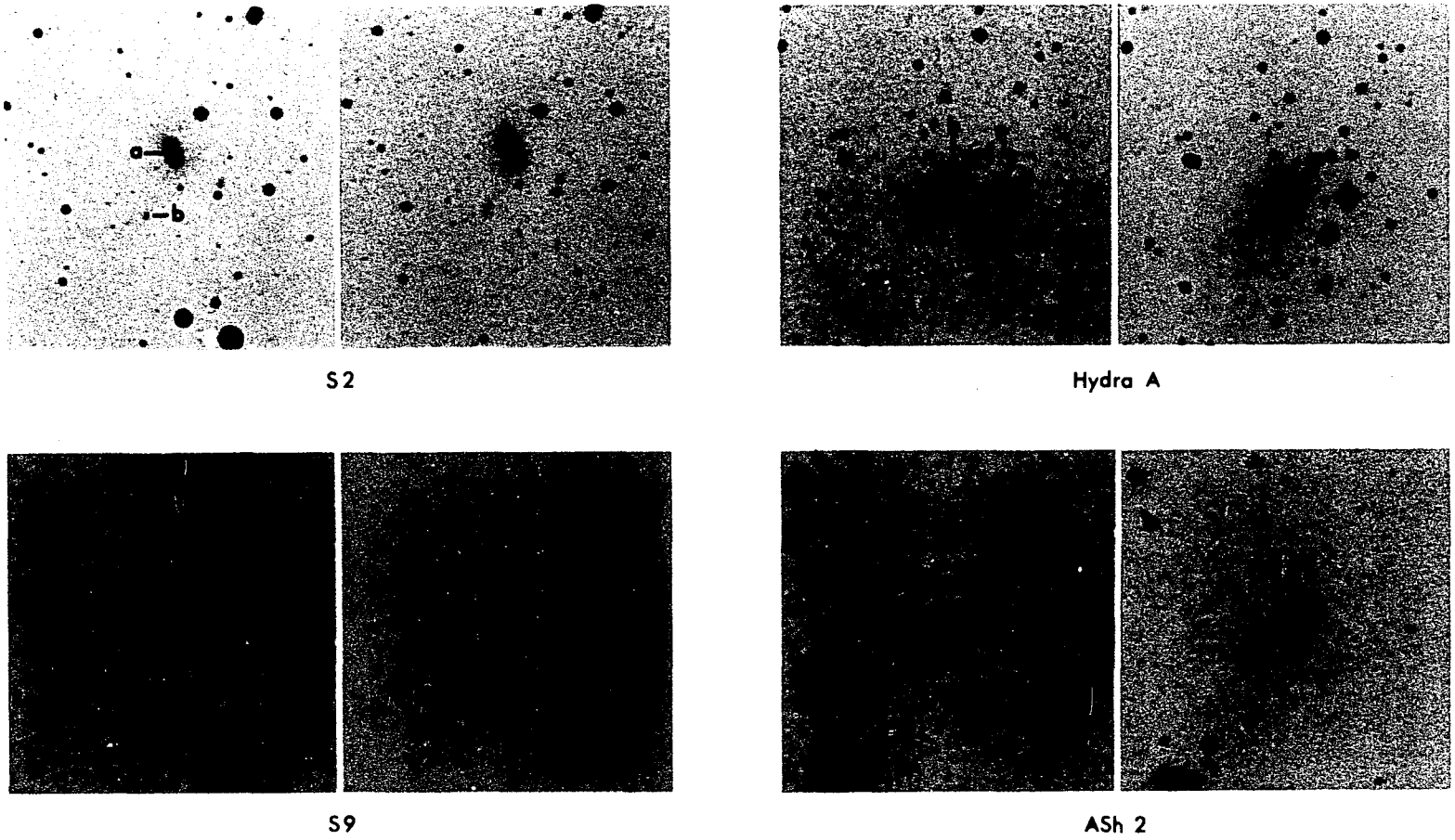

Fig. 1. Finding Charts for Blue Condensations Near Galaxies

The charts have been reproduced from the National Geographic-Palomar Observatory Sky Survey plates. In each pair the illustration from the blue-sensitive plate is on the left. North is at the top and west is to the right; the scale is 6.8"/mm.

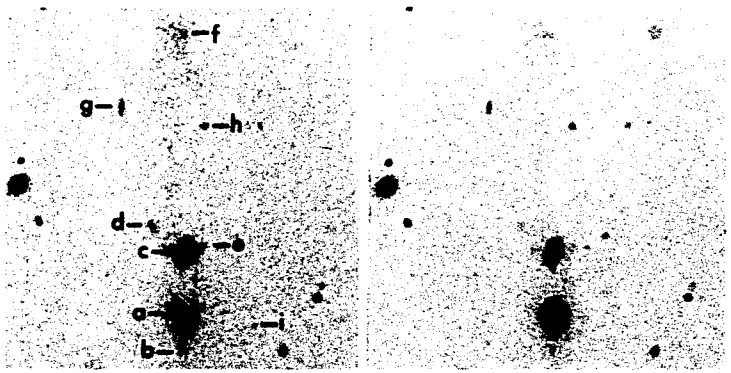

NGC 3561

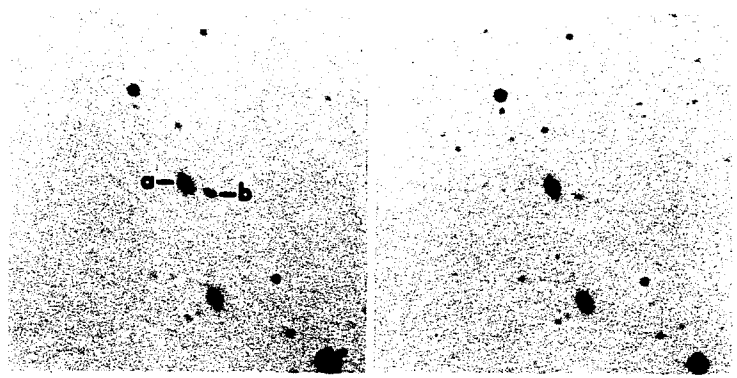

S 26

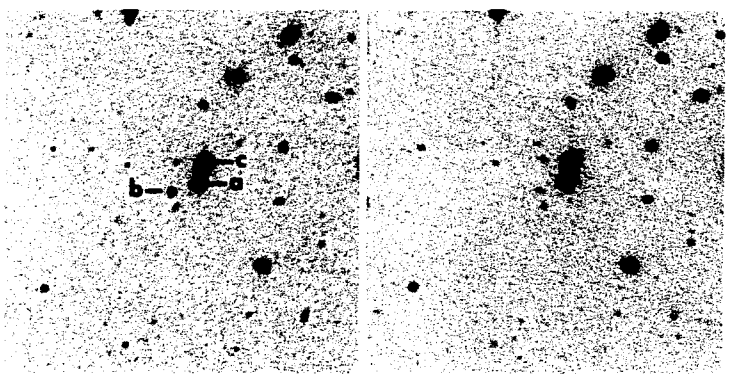

ASh 3

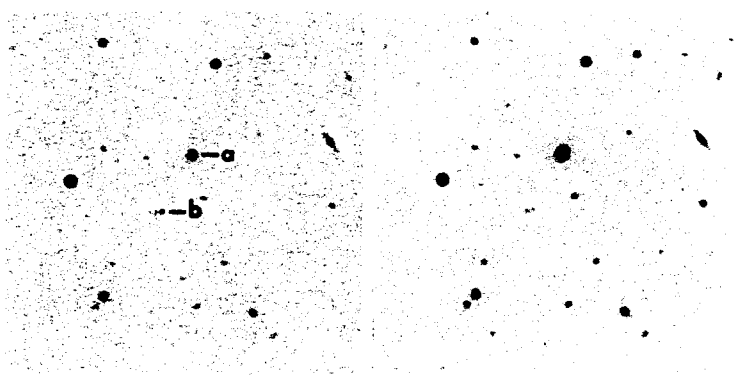

S 37

Fig. 1. Continued

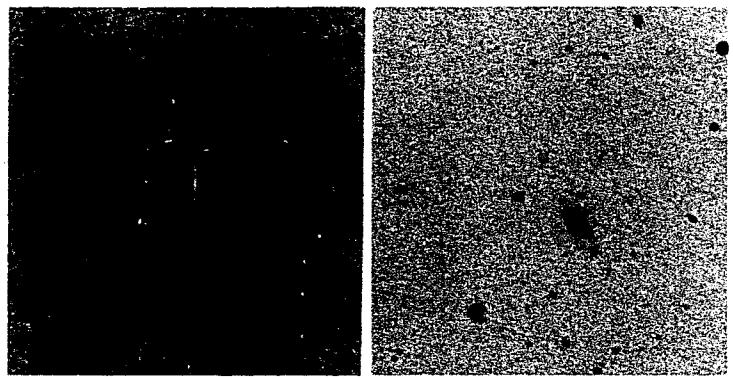

S 42

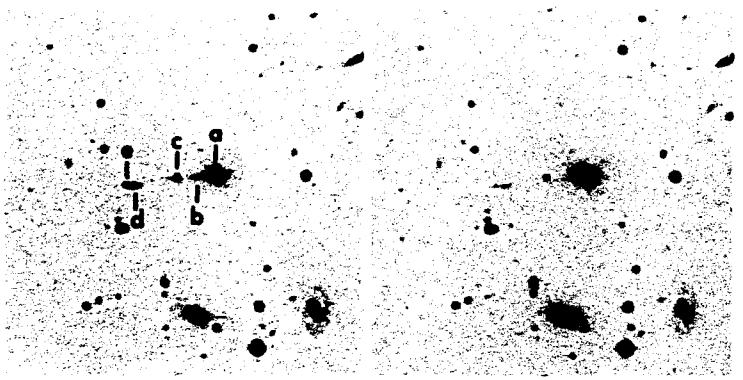

IC 1182

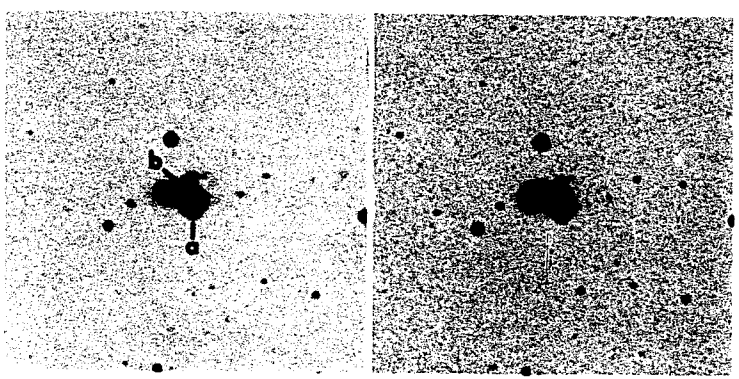

ASh 6

Fig. 1. Continued

Fig. 2. NGC 3561

This illustration, obtained with the Kitt Peak 84-inch telescope on baked Eastman Kodak IIIa-J emulsion, should be compared with the illustration of NGC 3561 in Figure 1. Notice especially the obscured regions on the south and west sides of the elliptical galaxy, the faint wisp at the south end of the bright condensation south of the elliptical galaxy, and the two condensations in the connecting jet.

Fig. 2. NGC 3561

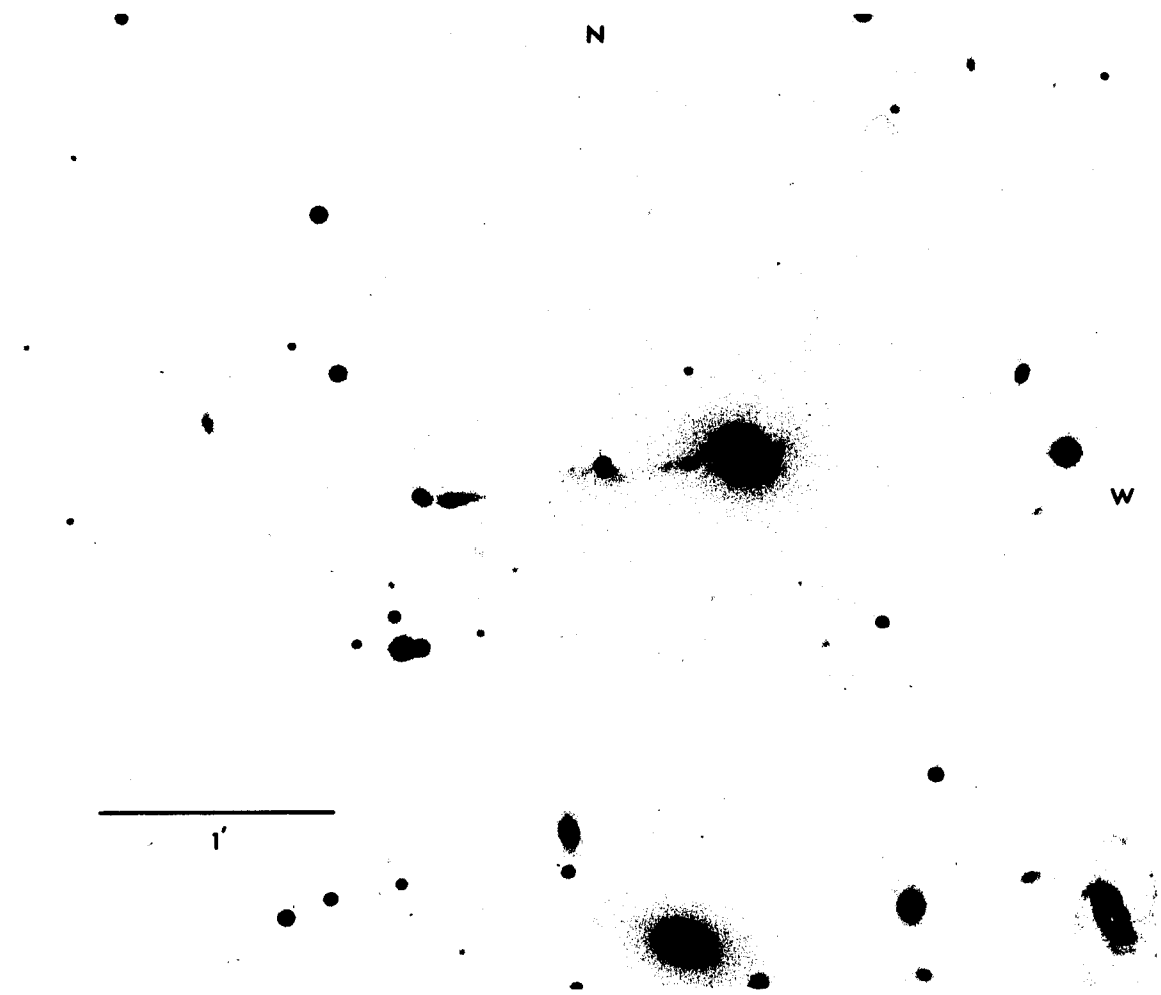

Fig. 3. IC 1182

This illustration is a reproduction from a plate obtained by Baade at the prime focus of the 200-inch telescope. Note the clustering of nebulosity about the stellar-appearing object near the center of the illustration. The diffuse material on the southwest side of IC 1182 itself (the bright galaxy to the right of center) has a large, faint extension to the north. (Photograph courtesy Mt. Wilson and Palomar Observatories.)

and the anonymous galaxies in the list of Ambartsumyan and Shachbazyan (1957). The following descriptions are based primarily on the appearance of the galaxies on the Sky Survey plates, supplemented in some cases by additional plate material obtained with the Steward Observatory 36-inch telescope and the Kitt Peak National Observatory 36-inch and 84-inch telescopes. The scales of these telescopes are 45, 29, and 13 "/mm, respectively. For those galaxies whose descriptions rely entirely upon the Sky Survey plates, the galaxy types are uncertain because the images are generally small and overexposed.

S 2. The Sky Survey plates show a uniform disc or body and a faint outer envelope; a short exposure 84-inch photograph shows that there is also a bright, nearly stellar nucleus. A straight feature projects outward near position angle 150°, apparently from a point just south of the nucleus. On the Sky Survey O-plate this feature can be traced to a blue condensation, which is slightly elongated in the same direction.

Hydra A. Ambartsumyan (1961) noted a blue starlike object about 30" north of the Hydra A radio galaxy. Although there are no similar objects within at least a 30'

radius of the radio galaxy, there is no direct evidence of any physical connection between the galaxy and the blue object.

S 9. This system is very similar to S 2. The galaxy has a nearly stellar nucleus, as seen on an 84-inch direct plate. A jet emerges from the central part of the galaxy near position angle 75^{o} and ends in an elongated blue condensation. There is also a faint blue stellar object about 40" southwest of the nucleus of the galaxy.

S 13. Although there is no obvious physical connection between this compact galaxy and the blue object to the west, there is a flaw on the Sky Survey O-plate very close to the region of interest. To the east of the galaxy there is some blue diffuse material, having two condensations and curving toward the north.

S 17. This is the brightest elliptical galaxy in a loose cluster. The blue object to the northeast of the galaxy appears to be stellar on a short exposure 84-inch photograph. There seems to be a blue linear feature leading from the galaxy about halfway to the blue object, but this feature is very subtle and may be a plate flaw. A bright spiral galaxy, apparently in physical association with the

elliptical galaxy, is directly opposite the blue object.

ASh 2. There are three blue objects in a line near this elliptical galaxy, but there is no evidence of a physical connection between any of them and the elliptical.

NGC 3561. The interesting features of this system were apparently first noticed by Ambartsumyan and Shachbazyan (1957). In addition to the reproductions from the Sky Survey plates shown in Figure 1, a photograph taken under good seeing conditions with the 84-inch telescope is shown in Figure 2. The galaxy labeled a in the illustration of NGC 3561 in Figure 1 is either a face-on S0 or an E0; there is considerable obscuration on the west and south sides (visible in Figure 2). Projecting southward from this galaxy is a jet having two nearly stellar, blue condensations and ending in a larger and brighter blue condensation b, which is slightly elongated in the direction of the jet. A small, faint wisp turns toward the west from the south end of this last condensation. Galaxy c is a peculiar spiral having diffuse blue extensions d and e. The large blue plume extending northward to two small condensations f seems to originate at the spiral galaxy. Whether or not g and h are associated with the system is not clear from the

photographic evidence alone; this statement applies also to the very blue 20th magnitude stellar object i.

S 26. This galaxy is similar to S 2 and S 9. There is, in this case, no visible physical connection between the galaxy and the blue object, although the blue object is substantially elongated in the direction of the nucleus of the galaxy. It is possible that the blue object is an unrelated galaxy; but its proximity and orientation, as well as its morphological similarity to other blue knots that are connected to their respective galaxies, argue against this interpretation.

ASh 3. These are two similar elliptical galaxies within a common envelope. Nearby there is a small blue galaxy, but there is no indication of a connecting bridge.

S 37. A blue stellar object southeast of this galaxy appears on the Sky Survey O-plate to have a very faint linear extension in the direction of the galaxy. This latter feature could very easily be a plate flaw; it has not been possible to obtain another long exposure photograph for confirmation.

Arp 196. Arp's 200-inch photograph of this system (Arp 1966) shows that the linear feature visible on the Sky

Survey plates actually forms a loop-like structure around the galaxy. Arp points out that this feature connects to the smaller galaxy to the south; but it also continues and connects with a blue galaxy even farther away. This system differs fundamentally from some of the others mentioned in that the bridge apparently does not connect to the nucleus of the elliptical galaxy.

S 42. There is a blue object very close to this elliptical galaxy. It is difficult to judge from the Sky Survey plates whether or not there is a connecting bridge between the two. In the same direction from the galaxy but approximately 1' from its center, there is another similar blue object. A large plume, very faint but similar to the one north of the spiral galaxy in the NGC 3561 system, extends from the galaxy on the side opposite to the blue condensations. There may also be a broad, diffuse bridge between S 42 and the nearby galaxy to the southeast.

S 48. Although there are no visible bridges between the galaxies, the arrangement of this system shows a striking similarity to that of NGC 3561: a spiral, an elliptical, and a small blue galaxy in a line. On a short-exposure 84-inch plate the spiral is seen to have a double nucleus.

IC 1182. This galaxy, described by Ambartsumyan and Shachbazyan (1957), is a member of the Hercules cluster. Burbidge and Burbidge (1961) have pointed out that the Hercules cluster and the Leo A cluster (of which NGC 3561 is a member) are rather similar in that they both contain a high proportion of spiral and irregular galaxies as well as a number of interacting systems. Figure 3 shows a 200-inch plate of the system taken by Baade. A blue linear structure, labeled b in the illustration in Figure 1, projects eastward from the elliptical galaxy a. This feature has an inflection near a star-like object c and continues in the direction of two elongated blue knots d and e. From the southwest side of the elliptical galaxy a faint, diffuse, S-shaped formation curves to the north.

Isolated Blue Galaxies

The second purpose of the search of the Sky Survey plates was that of finding relatively nearby individual galaxies whose color and morphological properties might be comparable to those of the blue knots discussed above. Two other surveys of blue galaxies were consulted: that of Haro (1956) and that of Markaryan (1967). Haro's list consists of 44 galaxies found on Tonantzintla Schmidt plates taken

for the purpose of discovering stars with large ultraviolet excesses. Three exposures were made on each plate, one each through yellow, blue, and ultraviolet filters, the images being slightly displaced from one another. This technique allowed objects having large ultraviolet excesses to be readily identified. The 70 galaxies in Markaryan's list were chosen from objects on objective prism Schmidt plates, mainly on the basis of the strength of their ultraviolet continua; four of the galaxies catalogued by Haro are included. Neither list is completely homogeneous in morphological type, but both contain a high proportion of galaxies that are rather compact and of moderately high surface brightness. These galaxies are often accompanied by faint irregular wisps of material. In these properties such galaxies quite closely resemble the blue knots associated with NGC 3561 and IC 1182.

From this group of galaxies Haro 4 (= Markaryan 36) was selected for detailed spectroscopic study. This galaxy, having colors B-V = 0.13, U-B = -0.64 (Hiltner and Iriarte 1958), is the bluest Haro galaxy for which photoelectric photometry is available. Three blue galaxies, brighter and of larger angular extent than most of the Haro and Markaryan

galaxies, were selected from those found in the survey with the blink comparator. Two (NGC 4190 and NGC 4485) are Magellanic irregulars; the third (NGC 4163) is rather difficult to classify but looks like a blue elliptical galaxy with a few bright O-B associations. Morgan (1959) has listed four galaxies--NGC 3395-6, NGC 3991, NGC 4214, and NGC 6052--that have exceptionally strong ultraviolet continua and emission-line spectra similar to that of the Orion Nebula; these galaxies have not been included in the present study.

Objective prism spectrograms taken by Haro and low dispersion slit spectrograms taken by Mayall (Haro 1956) show that the Haro galaxies generally have strong emission lines. Recently, DuPuy (1967, 1968) has studied some of these galaxies in more detail. The galaxies on Markaryan's list are currently being investigated at several observatories.

III

SPECTROSCOPIC OBSERVATIONS

All of the spectroscopic observations to be discussed in this chapter were made with the Kitt Peak 84-inch telescope Cassegrain spectrograph equipped with an image-tube camera. Observations during the late winter and the spring of 1967 were confined mostly to objects in published lists, as the survey described in Appendix I and in Chapter II had not yet been completed. The 1968 observations included published objects and some of those found recently by the author. Approximately half of the objects listed in Table 3 have not been observed at all; on the other hand, NGC 3561 and IC 1182 have been studied in some detail.

The Image-Tube Spectrograph

The Kitt Peak image-tube camera was developed by Dr. C. R. Lynds and has been used by him chiefly for investigating objects having stellar or nearly stellar images. In order to appreciate the reasons for some of the techniques applied, it is important to understand the characteristics of the specific equipment used for this study.

The image-tube apparatus, which replaces the photographic Schmidt camera on the conventional Cassegrain spectrograph, is shown in schematic form in Figure 4. The spectrum is imaged on the cathode of the image tube by a semi-solid Cassegrain Schmidt camera constructed of fused silica. The intensified image produced on the phosphor is re-imaged by means of a transfer lens (operating at unit magnification) onto a photographic plate. If the spectrum is to be widened, this is done by moving the plate in a direction perpendicular to the direction of dispersion rather than by trailing the object along the slit. This procedure has several advantages: (a) guiding is simplified, (b) a spectrogram can be made wider than the projected slit length, and (c) sky background can be reduced conveniently, because an entrance aperture only slightly larger than the image of the object may be used in place of a long slit. A disadvantage of moving the plate is that, if there are voids or other nonuniformities on the portion of the phosphor where the spectrum falls, such imperfections will appear on the final plate as spurious spectroscopic features.

Most of the spectrograms in this study were obtained with an English Electric Valve (EEV) P829D image tube. This

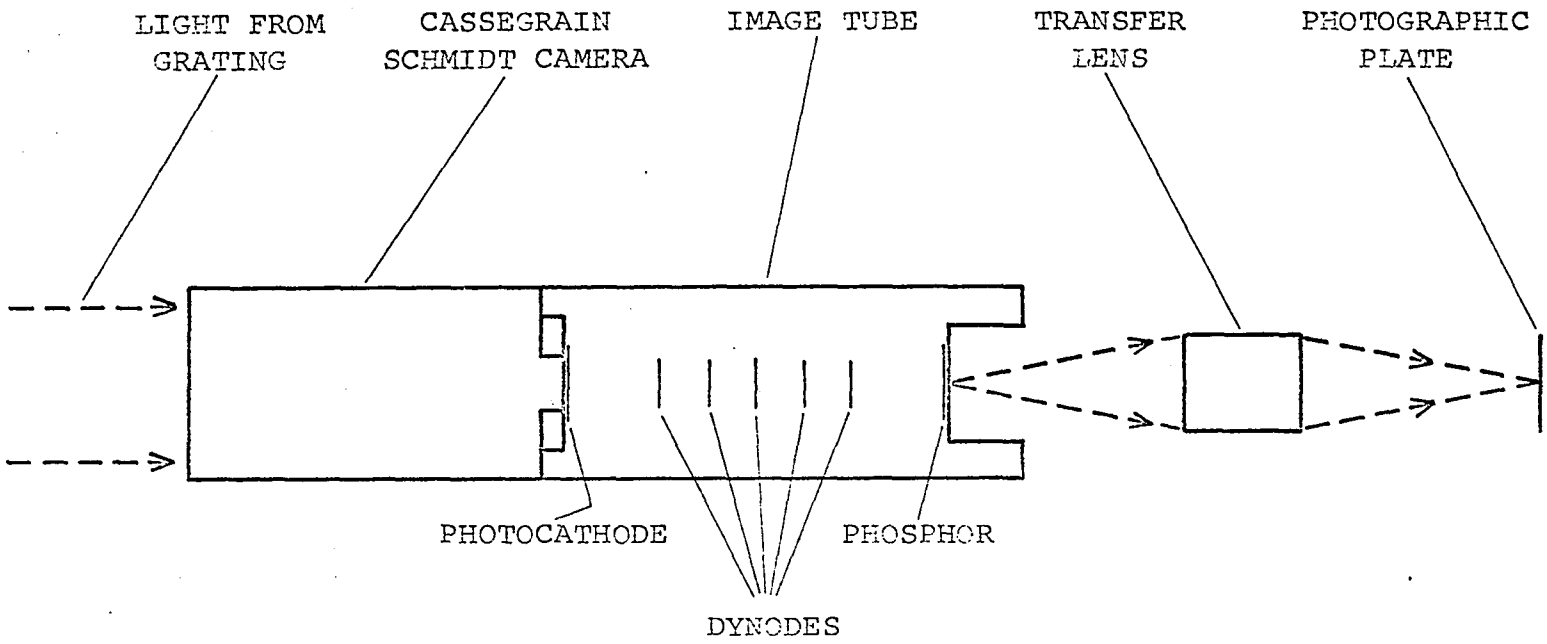

Fig. 4. Schematic Diagram of Image-Tube Camera

is a high-gain intensifier of the transmission-secondary-emission (TSE) type, having six stages. [Baum (1967) has given a brief review and description of the various types of image tubes that have found uses in astronomy.] A general characteristic of TSE intensifiers is that the distribution function of brightnesses for the phosphor scintillations is very broad; this is primarily due to statistical fluctuations in the number of secondary electrons produced at the first dynode.

If the full potential of the image tube is to be realized, the faintest scintillations must be recorded. However, because of the wide range of scintillation brightnesses, high photographic densities will normally be reached at low information densities. There are two ways to achieve a high total information content for a spectrogram: one may accept the low information density and make the spectrum very wide, or one may use some method of recording all scintillations weakly and with approximately equal weight. Both approaches have been used in this investigation. Spectra of objects for which resolution along the slit was unimportant were widened and the spectrograms were developed in D-19 or D-76. For all widened spectrograms the unused

portions of the phosphor were masked off in order to reduce the number of image-tube background scintillations recorded on the photographic plate. Certain plates, on which it was necessary to preserve resolution along the slit, were processed in a low-contrast, wide-latitude developer (POTA), described by Lutnes and Davidson (1966).

A few of the spectrograms were obtained using a three-stage cascaded image tube (henceforth called the ICL intensifier) developed and built by Dr. J. D. McGee and his associates at Imperial College, London. The ICL intensifier has a lower total light gain than the EEV P829D and is most suitable for unwidened spectrograms.

Nearly all magnetically focused image tubes suffer somewhat from S-distortion. If a straight line is imaged on the photocathode, the line seen on the phosphor will have an "S" shape; this effect is due to slight nonuniformities in the magnetic field. Although S-distortion is fairly severe for the EEV intensifier, the spectral lines themselves are not curved when the spectrum is widened by moving the plate. There are, however, certain geometrical distortions produced by the image tube that show up as irregularities in the dispersion curve. Whenever a spectral line of an object

falls in a region of the spectrum where there are too few comparison lines to clearly define the dispersion curve, the wavelength of the line in the spectrum of the object is subject to somewhat larger uncertainties than would be the case for a conventional photographic spectrogram having the same resolution.

Discussion of Spectroscopic Observations

Reference should be made to Figures 1, 2, and 3 in Chapter II for illustrations of objects discussed in this section. The lower-case letters used in the discussion refer to the designations on the identification charts in Figure 1. Table 4 gives basic data for certain of the spectrograms obtained for this study. Velocities are corrected to the local standard of rest assuming a solar motion of 300 km/sec toward $l^{II} = 90^{o}$, $b^{II} = 0^{o}$ unless otherwise stated. This solar motion is the same as that used in the redshift catalogue of Humason, Mayall, and Sandage (1956) and in recent papers by Schmidt (1965) and Sandage (1966).

NGC 3561

Spectroscopic observations of this system have been restricted to the two bright galaxies a and c, the blue

Table 4 List of Spectroscopic Plates

Eastman Kodak IIa-O plates were used for all spectrograms. Trailed spectrograms are indicated by a letter T in the exposure column. All untrailed spectrograms taken with the EEV intensifier were developed in POTA low-contrast developer; all others were developed in D-19 or D-76.

Object	Plate Number	Image Tube	Nominal Resolution	Wavelength Range	Exposure (minutes)	
S 2						
a,b	CI 620	EEV	5 Å	3100-5100Å	30	
a	625	EEV	10	3100-7700	15	T
Hydra A						
a,b	383	ICL	8	3100-5800	30	
b	389	EEV	10	3100-7700	75	T
b	637	EEV	10	3100-7700	70	T
ASh 6						
a	626	EEV	10	3100-7700	5[a]	T
b	627	EEV	10	3100-7700	30 object	T
					15 sky	
S 9						
b	622.1	EEV	10	3100-7700	105	T
a	622.2	EEV	10	3100-7700	21	T
a,b	638	EEV	1.5	3100-4150[b]	30	
Haro 4	618	EEV	10	3100-7700	24 object	T
					12 sky	
	633	EEV	1.5	3100-4150[b]	15	
	698	EEV	1.5	3500-4550	90[a] object	T
					30 sky	
NGC 3550	396	EEV	5	3100-5800	60	T

Table 4 Continued

Object	Plate Number	Image Tube	Nominal Resolution	Wavelength Range	Exposure (minutes)	
ASh 2						
b,c,d	CI 385	ICL	8 Å	3100-5800Å	30	
a,b	386	ICL	8	3100-5800	20	
b	395	EEV	5	3100-5800	42	object T
					21	sky
NGC 3561						
a,b,c	376	ICL	8	3100-5800	40	
i	391	EEV	10	3100-7700	135	T
b	617	EEV	10	3100-7700	112	object T
					56	sky
a,b,c	629	EEV	10	3100-7700[b]	15	
a,b,c	630	EEV	1.5	3100-4150	60	
ASh 3						
b	428.1	EEV	5	3100-5800	60	T
a	428.2	EEV	5	3100-5800[b]	20	T
NGC 4485	639.1	EEV	1.5	3100-4150[b]	15	
NGC 4190	639.2	EEV	1.5	3100-4150[b]	10	
NGC 4163	639.3	EEV	1.5	3100-4150[b]	10	
S 37						
b	624	EEV	10	3100-7700	60	T
a	632	EEV	10	3100-7700[b]	15	T
a,b	640	EEV	1.5	3100-4150	30	
IC 1182						
a,b,c,d,e	380	ICL	8	3100-5800	30	
e	393	EEV	5	3100-5800	60	T
c	397	EEV	5	3100-5800	50	T

Table 4 Continued

Object	Plate Number	Image Tube	Nominal Resolution	Wavelength Range	Exposure (minutes)	
IC 1182						
e	CI 432	EEV	5 Å	3100-5800Å	75	T
c	433	EEV	10	3100-7700	30	T
a	488	EEV	10	3100-7700	55	T
b	619	EEV	1.5	3100-4150[b]	90[a]	T
a,b,c,d,e	634	EEV	1.5	3100-4150[b]	60	
Saakyan						
Galaxy	398	EEV	5	3100-5800	30	T
b	429	EEV	5	3100-5800	60	T
NGC 2392	615[c]	EEV	10	3100-7700	30[a]	T
HD 86986	616[c]	EEV	10	3100-7700	30[a]	T

a. Filter used: CI 626--$2^m.5$ neutral, CI 698--BG 12, CI 619--BG 12, CI 615--$2^m.5$ neutral, CI 616--$7^m.5$ neutral.

b. Both the first-order red and the second-order ultraviolet were recorded. Data is given for the second order.

c. Calibration plates.

knot b south of the elliptical galaxy, and the faint blue star-like object i. Because a, b, and c are nearly in line, all three objects may be placed on the slit at the same time. Zwicky's spectrogram, described in Chapter I, was obtained in this manner.

The sensitivity of Zwicky's spectrogram did not extend beyond about 4900 Å, and the only feature seen in the spectrum of the blue knot b was [O II] λ3727. Accordingly, a spectrogram (CI 376) covering the range from 3100 Å to 5800 Å was obtained, using the ICL 3-stage cascaded intensifier. This spectrogram and a similar one of IC 1182 (CI 380) have been briefly discussed elsewhere (Stockton 1968). The emission spectrum of the blue knot b is qualitatively similar to that of a diffuse emission nebula, Hβ being in this case somewhat stronger than [O III] λ4959 but considerably weaker than [O III] λ5007. In addition to the [O II] λ3727 doublet in emission and the absorption lines found by Zwicky in both of the bright galaxies, there is strong Hβ emission and a very weak [O III] λ5007 line in the spectrum of the spiral galaxy. The elliptical galaxy shows only a weak [O III] λ5007 line. The recorded continuum of the elliptical galaxy appears to have its maximum density near

Hβ, whereas that of the blue knot b has its maximum somewhere near 4000 Å. It is, therefore, apparent that the blue color of the knot cannot be entirely explained by the strength of the [O II] λ3727 doublet.

A low dispersion widened spectrogram (CI 617) of the blue knot b, which was obtained for the purpose of determining the spectral-energy distribution (see the section on spectrophotometry in this chapter), was searched unsuccessfully for absorption lines.

Finally, a high resolution unwidened spectrogram (CI 630, Fig. 5) was taken of objects a, b, and c, using the EEV image tube. The plate was developed in modified POTA low-gamma developer. For this spectrogram the grating was placed in a manner such that both first-order Hα and second-order [O II] λ3727 were recorded. The resolution in second-order is about 1.5 Å.

The [O II] λ3727 doublet in the spiral galaxy c is much less evident on this plate than on the lower dispersion spectrogram (CI 376); the effect is probably partly a result of the use of the low-contrast developer. In the spectrum of the elliptical galaxy a the blended [O II] λ3727 doublet, although broad, is easily visible and indicates a velocity

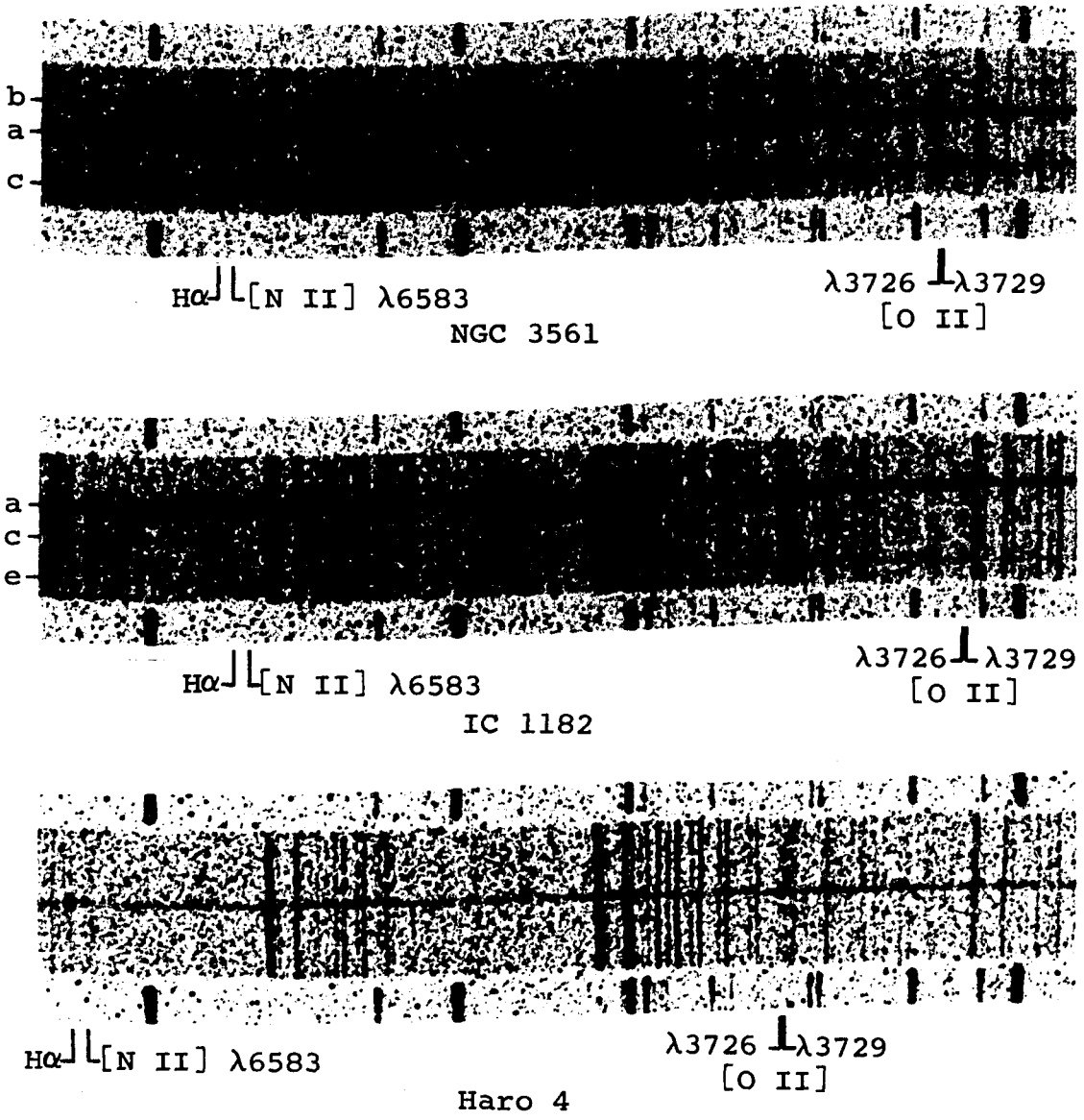

Fig. 5. Spectrograms of NGC 3561, IC 1182, and Haro 4

All three spectrograms were obtained with the grating set so that both Hα in the first order and the [O II] doublet in the second order were recorded. In several of the objects the [O II] λ3727 doublet is resolved. The faint Hα emission between objects (a) and (c) in the IC 1182 spectrogram has the same velocity as the contiguous part of the highly inclined Hα line in the galaxy (a). Note the strength of Hα compared to [N II] λ6583 in Haro 4.

dispersion for the gas in the nucleus of the elliptical of a few hundred km/sec. On the other hand, the components of the doublet are clearly resolved in the spectrum of the blue knot b, and from the width of the lines it is possible to put an upper limit of about 80 km/sec on the internal velocity dispersion of the gas. The λ3727 doublet is also resolved in the two faint blue condensations (Zwicky 1956) in the bridge between the elliptical galaxy a and the blue knot b; however, in one of the faint condensations only the longward component is visible. Finally, the λ3727 doublet appears to be present and resolved in some very faint diffuse material about halfway between galaxies a and c.

In the blue knot b the two components of the [O II] λ3727 doublet are nearly equal in intensity. Using the well-known relationship between the intensity ratio of these lines and the electron density in the form given by Seaton and Osterbrock (1957) and assuming an electron temperature of 10 000 ^{o}K, we find the electron density to be about 700 cm^{-3}. The electron density seems to be somewhat lower in the two faint blue condensations, but grain statistics prevent a precise determination.

The lines Hα and [N II] λ6583 both appear in the spectrum of the spiral galaxy c; Hα is somewhat the stronger. In the spectrum of the blue knot b, Hα is at least three times as intense as λ6583. A curious characteristic of the Hα line in the bridge between the elliptical galaxy a and the blue knot b is that the line is uniform in intensity for about half of the distance (the region nearest to the blue knot), whereas the [O II] emission comes from discrete condensations in this same region of space.

NGC 3561 belongs to a fairly rich, somewhat irregular cluster of galaxies which Zwicky calls the Leo A cluster. Spectrograms of two other galaxies in this cluster have been obtained in the present study. The spectrum of one of these, ASh 2, will be described below. The other galaxy, NGC 3550, is northwest of NGC 3561 and has a double nucleus. Averaging the velocities for these galaxies with the average of the velocities for the spiral and elliptical components of NGC 3561 gives a value of 9813 km/sec for the cluster (Table 5).

With an adopted Hubble constant of 75 km/sec/Mpc, this radial velocity corresponds to a distance of 131 Mpc.

Table 6 gives certain physical data for the components of NGC 3561 assuming this distance.

Table 5 Radial Velocity of the Leo A Cluster

Galaxy	Velocity
NGC 3561	8669 km/sec
NGC 3550	10430
ASh 2	10340
Average for Cluster	9813 km/sec

With the values obtained for the separations and radial velocities of the galaxies, it is possible to make some comments concerning the dynamics of the system. In order that two bodies be gravitationally bound, it is necessary that

$$v_{12} < w_{12} = \left[\frac{2G(M_1 + M_2)}{R_{12}}\right]^{1/2}$$

where w_{12} is the upper limit to the relative velocity if the system is to be gravitationally bound, v_{12} is the actual relative velocity of the two bodies, R_{12} is their separation, and M_1 and M_2 are their respective masses. Because of projection effects, it is possible to measure only the line-of-sight component of the velocity and the transverse

Table 6 Physical Data for the NGC 3561 System

A Hubble constant of 75 km/sec/Mpc has been assumed, and a cluster redshift of 9857 km/sec, derived from the redshifts of three member galaxies, has been used. The apparent photographic magnitudes have been taken from Zwicky and Humason (1961); the various angular dimensions have been measured from a plate taken with the Kitt Peak 84-inch telescope.

Object	V_r	Dimensions	angular	linear	Separation	angular	linear	m_{pg}	M_{pg}
Spiral (c)	8802 km/sec	$\Delta\alpha$	13".7	8.7 kpc				$14^m.7$	$-20^m.9$
		$\Delta\delta$	26.1	16.6					
					56".8	36.1 kpc			
Elliptical (a)	8535	$\Delta\alpha$	16.3	10.4				14.4	-21.3
		$\Delta\delta$	14.5	9.2					
					31.3	19.9			
Blue Knot (c)	8895	$\Delta\alpha$	3.2	2.0				18.5	-17.1
		$\Delta\delta$	4.0	2.5					

component of the separation. If the masses are known, an upper limit to the dissociation velocity w_{12} can be found by using R'_{12}, the projection of the separation R_{12}. It will be assumed here that galaxies a and c have masses of $10^{12}\odot$, that the mass of the blue knot b is negligible by comparison, and that the influence of the spiral galaxy on the motion of the blue knot may be neglected. Then for galaxies a and c

$$w_{ac} \leq \left[\frac{2G(M_a + M_c)}{R'_{ac}}\right]^{1/2} \approx 700 \text{ km/sec.}$$

For the elliptical galaxy a and the blue knot b

$$w_{ab} \leq \left[\frac{2G\ M_a}{R'_{ab}}\right]^{1/2} \approx 700 \text{ km/sec.}$$

If we suppose that the blue knot b is moving radially outward from the nucleus of the elliptical galaxy, an additional constraint is placed on the magnitude of the relative velocity v_{ab} for the system to remain bound. Let φ be the angle of the velocity vector with respect to the line of sight; then the radial velocity difference $\Delta v_r = v_{ab} \cos \varphi$, and the projected separation $R'_{ab} = R_{ab} \sin \varphi$.

Then for a gravitationally bound system

$$\left|\Delta v_r \sec \varphi\right| < \left[\frac{2G\ M_a}{R'_{ab} \csc \varphi}\right]^{1/2},$$

$$\Delta v_r < \left|\cos \varphi\right| \left[\frac{2G\ M_a \sin \varphi}{R'_{ab}}\right]^{1/2},$$

$$\Delta v_r < \left(\left|\cos \varphi\right| \sin^{1/2}\varphi\right)\ 700 \text{ km/sec}.$$

The expression $\left|\cos \varphi\right| \sin^{1/2}\varphi$ has a maximum at $\varphi = \pi/4$, where its value is approximately 0.6. Thus if the system is bound, the maximum value of Δv_r is 420 km/sec. The most probable value of φ is 60° for which Δv_r = 330 km/sec; the observed value of Δv_r is 360 km/sec. If the velocity vector of the blue knot is not radial with respect to the elliptical galaxy, little can be said from the spectroscopic observations concerning the stability of the system. However, if the blue knot b, the two fainter condensations, and their connecting material actually form a linear structure, this structure itself almost certainly cannot be stable under gravitational forces alone for a time of the order of an orbital period about the elliptical galaxy a, i.e. a few times 10^8 years.

The 20th magnitude blue stellar object i was noticed while the Sky Survey O- and E-plates were being compared.

Because of its proximity to NGC 3561 and its extremely blue color, it was felt that this object might bear some relation to the other blue knots associated with this system. A spectrogram (CI 391), however, showed it to be a quasi-stellar object (QSO) with a redshift $z = \Delta\lambda/\lambda = 2.195$. It is interesting that Zwicky (1967b) has selected the Leo A cluster as one that might profitably be searched for compact objects having significant gravitational redshifts; but, in the absence of any convincing evidence that the QSO is associated with the cluster or with NGC 3561 in particular, it seems most reasonable to regard the coincidence with the galaxy as fortuitious. Sandage and Luyten (1967) have estimated that there are from 1 to 3 QSOs brighter than magnitude 19.7 per square degree, and there is recent evidence (Braccesi, Lynds, and Sandage 1968) that this estimate may be conservative. The probability that a faint QSO should be found near some part of a system having the angular extent of NGC 3561 is, therefore, not negligible.

IC 1182

This system is one of a number of unusual galaxies to be found in the Hercules cluster of galaxies. Table 7

Table 7 Physical Data for the IC 1182 System

A Hubble constant of 75 km/sec/Mpc has been assumed, and a cluster redshift of 10 775 km/sec (Burbidge and Burbidge 1959) has been used. The apparent photographic magnitude estimates are from Ambartsumyan and Shachbazyan (1957); the angular dimensions were measured on a plate taken with the Kitt Peak 84-inch telescope.

Object	V_r	Dimensions			Distance From Galaxy		m_{pg}	M_{pg}
			angular	linear	angular	linear		
Galaxy (a)	10292 km/sec	$\Delta\alpha$	14".7	10.3 kpc	--	--	$15^m.5$	$-20^m.3$
		$\Delta\delta$	12.6	8.8				
Blue Knot (d)	10085	$\Delta\alpha$	8.0	5.6	74".2	51.8 kpc	19.0	-16.8
		$\Delta\delta$	3.3	2.3				
Blue Knot (e)	10091	$\Delta\alpha$	4.7	3.3	81.3	56.7	19.4	-16.4
		$\Delta\delta$	4.0	2.8				

gives certain physical parameters for IC 1182 and the two brightest blue knots associated with it.

When the spectrograph slit is placed through the center of the main galaxy a and the mean position of the two blue knots d and e, it also admits the faint condensations at b and some of the nebulosity near the star-like object c. A spectrogram (CI 380) was taken with the slit in this position, using the ICL cascaded tube and covering the spectrum from 3100 Å to 5800 Å. The emission lines [O II] λ3727, Hβ, and [O III] λ5007 are seen in all five objects. In addition to these lines, the outer blue knot e shows Hγ and [O III] λ4959; and the galaxy a shows [O III] λ4959, [Ne III] λ3869, and the Balmer series through Hζ. The spectrum of the outer knot e very closely resembles that of the blue knot associated with NGC 3561 both in the relative emission line strengths and in the spectral-energy distribution.

A second untrailed spectrogram (CI 634, Fig. 5) was obtained with the same instrumental configuration as that used for the high resolution spectrogram (CI 630) of NGC 3561. The tilt of the Hα line in the galaxy a gives a velocity difference of 430 km/sec over a distance of 9", in

fairly good agreement with the value 350 km/sec over a distance of 8" determined by Burbidge et al. (1963) for a similar slit position. Other lines seen in emission in the spectrum are [N II] λλ6548, 6583 (λ6583 is considerably weaker than Hα), and [S II] λλ6716, 6731. In the region between galaxy a and the nebulosity near c the Hα emission is uniformly distributed; in contrast, the [O II] λ3727 emission comes from discrete knots. This is the same effect that was found for the connecting bridge in the NGC 3561 system. The Hα emission line in the bridge of IC 1182 joins the highly inclined Hα line in the galaxy a. Thus, there is continuity between the velocity fields of the gas in the rapidly rotating outer part of the galaxy and the gas in the bridge.

Only the long-wavelength component of the [O II] λ3727 doublet is visible in the spectra of the condensations at b, the nebulosity near c, and the condensation d. Both components appear in the spectrum of condensation e, the λ3729 component being slightly the stronger. Although the line ratios on this plate cannot be accurately determined, an estimate gives an intensity ratio of about 1.1 and an electron density of about 500 cm^{-3} in condensation e. In

the nebulosity near c and in the condensations b and d the electron density is probably less than 200 cm^{-3}. Spectrograms similar to CI 630 and CI 634 were obtained of the planetary nebula IC 418 and of a region in the Orion Nebula. As the intensity ratio of the [O II] λ3727 doublet is known for both objects, these spectrograms provided rough standards by which the intensity ratios in the other objects could be estimated.

The relationship between the morphological and dynamical characteristics of this system deserves some comment. From its apparent form and color it is reasonable to classify IC 1182 as an elliptical galaxy. This description, however, must be strongly qualified by several peculiarities: (a) the presence of strong emission lines, not only in the nucleus, but over a region six kiloparsecs in diameter (assuming a Hubble constant of 75 km/sec/Mpc); (b) a ratio of intensities of Hα to [N II] λ6583 of about 3 [in a sample of elliptical galaxies observed by Burbidge and Burbidge (1965) no ratio higher than 1 was observed]; (c) a substantial velocity gradient across the galaxy although the projected image of the galaxy is not greatly flattened; and (d) the assymmetrical distribution of diffuse material near

the galaxy. The ratio of the minor to the major axis of the bright, regular part of the galaxy is about 0.85. If it is assumed that the galaxy is actually a flattened system having an inclination φ to the plane of the sky so that cos φ = 0.85 and if the tilt of the spectral lines is interpreted as due to rotation, then the true rotational velocity v_o = v_m csc φ, where v_m is half of the total velocity difference indicated by the lines. In this case v_m = 215 km/sec and $\varphi = 32^o$, so v_o = 405 km/sec. This value is to be compared with the velocity of escape v_e at this distance R from the center of the galaxy,

$$v_e = \left(\frac{2GM}{R}\right)^{1/2},$$

where M is the mass of the galaxy contained within the radius R. R is 3 kiloparsecs, and we assume M to be of the order of 10^{11} M (probably an overestimate). Then $v_e \approx$ 400 km/sec.

Although the close similarity of v_o and v_e is no doubt fortuitious, the hypothesis that the gas in this galaxy is rotationally unstable is attractive. It would tend to explain not only the peculiarities mentioned above but also the fact that all of the material east of the galaxy

has a velocity of the same sign with respect to the center of the galaxy.

Several widened spectrograms of individual objects in the system have been obtained. The two widened spectrograms (CI 393 and CI 432) of object e were searched unsuccessfully for absorption lines. The two spectrograms (CI 397 and CI 433) of the stellar object c show a featureless spectrum. This object is not especially blue; hence the absence of detectable spectral features cannot be explained by supposing it to be an early type star having only weak absorption lines. This evidence, taken together with the geometry of the nearby nebulosity (see Fig. 3), indicates that c is not a foreground star but is a compact galaxy associated with IC 1182.

S 2

Two spectrograms were obtained: one (CI 620) was widened with the slit placed through the galaxy a and the blue condensation b; the other (CI 625) was a widened spectrogram of the galaxy. Unfortunately, this system was quite far west when these spectrograms were taken, and neither of the plates is of satisfactory quality. The only convincing spectral feature seen on either spectrogram was

a weak emission line at 6693 Å in the spectrum of the galaxy. If this line is Hα, the radial velocity is 6180 km/sec.

Hydra A

The blue object b found by Ambartsumyan (1961) north of galaxy a (identified with the Hydra A radio source) has an angular diameter of less than 3". An unwidened spectrogram (CI 383) obtained with the spectrograph slit passing through a and b shows strong [O II] λ3727 emission and a few weaker emission features in the spectrum of the galaxy but only a blue continuous spectrum for object b. The radial velocity for the galaxy agrees with the value of 15 900 km/sec given by Minkowski (1961). A widened spectrogram (CI 389) of object b seems to show a few weak absorption features, some of which are confirmed by an additional spectrogram (CI 637). There appears to have been a change in the spectrum between these last two plates, for CI 637 shows several spectral features that were not seen on CI 389 but which, nevertheless, seem to be real. The only spectral lines that can be identified are Hβ, Hγ, and Hδ in absorption. Hβ and Hγ are seen to be double, the shorter wavelength component being the stronger and having the same

Table 8 Redshifts of Program Objects

All values are corrected to the local standard of rest, assuming a solar velocity of 300 km/sec towards $l = 90^{\circ}$, $b = 0^{\circ}$. The redshift parameter z is defined by $z = (\lambda - \lambda_o)/\lambda_o$, where λ and λ_o are, respectively, the observed and rest wavelengths for a spectral feature.

Object	z	V_r
S 2 (a)	(0.0206)	(6180) km/sec
ASh 6 (b)	0.0212	6360
S 9 (a)	0.0521	15620
(b)	0.0522	15650
Haro 4	0.00194	582
NGC 3550	0.0348	10430
NGC 3561 (a)	0.02847	8535
(b)	0.02967	8895
(c)	0.02936	8802
(i)	2.195	--
ASh 2 (a)	0.0345	10340
(b)	0.0318	9530
ASh 3 (a)	0.0498	14930
(b)	0.0432	12950
S 37 (b)	2.036	--
IC 1182 (a)	0.03431	10292
(b)	0.03365	10088
(c)	0.03373*	10112*
(d)	0.03364	10085
(e)	0.03366	10091
Saakyan Galaxy	0.0365	10942

* The redshift refers to the nebulosity.

velocity as the Hδ line--about +525 km/sec (not corrected for galactic rotation). The weaker component of Hβ and Hγ has a velocity of +2260 km/sec. Both of these velocities are much smaller than that of the Hydra A radio galaxy. Several unidentified absorption features are present, the strongest being at 4037 Å and 4175 Å. There is also a complex feature between 4600 Å and 4700 Å.

Corrected for galactic rotation, the two velocities for the hydrogen lines become +283 km/sec and +2018 km/sec. The second of these velocities is far above the velocity of escape for the Galaxy. Therefore, it seems most reasonable to regard the object as extra-galactic; but, in any case, it almost certainly cannot be associated with the Hydra A galaxy. Although the object is extremely interesting in itself, it apparently does not fall within the defined area of the present study.

S 9

The blue object b is slightly elongated and is connected to the galaxy a by a thin filament. Plate CI 622 contains widened spectra of both the galaxy and the blue knot. The galaxy shows [O II] λ3727 emission, and the H and K lines of Ca II and the G band in absorption; the blue knot

shows [O II] λ3727, [Ne III] λ3869, Hβ, and [O III] λ5007 in emission and extremely weak H and K in absorption. There is a very marked difference between the continua of the two objects: the exposures are such that the continuum densities are approximately equal at about 5000 Å, whereas at 4000 Å the continuum of the blue knot is recorded with about three times the density of that of the galaxy.

ASh 2

This system is a member of the Leo A cluster, to which NGC 3561 also belongs. Of the three blue objects present, the brightest (b) has a non-stellar image on an 84-inch direct photograph on which the smallest stellar images correspond to slightly less than 2"; the other two blue objects (c and d) have stellar images. For one spectrogram (CI 385) the slit was placed through the three blue objects. Object b shows a strong [O II] λ3727 emission line and weaker [O III] λ5007 and Hβ emission. Objects c and d show blue continua only. The features seen in the spectrum of b were confirmed on another spectrogram (CI 386) for which the slit was placed through the galaxy a and the blue knot b. The spectrum of the galaxy shows absorption in H and K of Ca II and the G band but no emission lines. A widened spectrogram

(CI 395) of b was searched unsuccessfully for absorption lines.

An analysis similar to that carried out for NGC 3561 indicates that, with a velocity difference of about 800 km/sec between the galaxy and blue knot b, the two cannot form a bound system.

ASh 3

This system is a member of the Leo B cluster. The blue object b has a non-stellar image and is close to a pair of elliptical galaxies a and c having a common envelope. Plate CI 428 contains widened spectra of both the blue knot b and the southernmost (a) of the two elliptical galaxies. Preliminary results from this plate have been reported by Zwicky (1967b, 1967c). The spectrum of the elliptical galaxy a shows only the absorption lines H and K of Ca II and the G band. The spectrum of the blue knot has strong [O II] λ3727 emission, and weak H and K absorption lines. Once again, a large velocity difference (in this case 2000 km/sec) eliminates the possibility that the galaxy (a) and the blue knot b are gravitationally bound to each other. The evidence bearing on the relation of the blue knots to the galaxies ASh 2 and ASh 3 will be discussed in Chapter IV.

S 37

The blue object b has a stellar appearance on an 84-inch direct photograph; the upper limit to the angular size is about 2". On the Sky Survey O-plate a very subtle filament is seen extending from the blue object in the general direction of galaxy a. There is no evidence at all for this feature on the E-plate, and it could easily be a plate flaw. A short exposure widened spectrogram (CI 632) of galaxy a shows no emission lines; the continuum is not exposed well enough to show absorption lines.

A widened spectrogram of the blue object b shows three prominent emission features that can be satisfactorily identified with Ly-α, C II λ1335, and C IV λ1549. The mean redshift for these lines is 2.036. Once again, in the absence of any convincing external argument relating quasi-stellar objects and galaxies, it seems most reasonable to regard this proximity as a chance occurrence.

Saakyan Galaxy

Saakyan (1965) has described two blue stellar objects in the vicinity of an elliptical galaxy. The objects are very similar: both have photographic magnitudes of about 18.2 and color indices (international system) of

about $-0^{m}.5$. Because no other objects of this description were found within a radius of 10', Saakyan suggested that they might have some relation to the galaxy.

A spectrogram (CI 398) of the galaxy shows the absorption lines H and K of Ca II but no emission lines. A spectrogram (CI 429) of one of the blue objects (labeled b on Saakyan's finding chart) shows it to be a star with broad hydrogen absorption lines. Hβ may have weak central emission. The other blue object was not observed.

Haro 4

The list of blue galaxies given by Haro (1956) was compiled from a series of plates on which slightly displaced images in yellow, blue, and ultraviolet light had been impressed. Haro 4 is one of the most "violet" of these galaxies; photoelectric photometry by Hiltner and Iriarte (1958) gives B-V = 0.13 and U-B = -0.64. An 84-inch direct plate shows a slightly elongated bright central region and a fainter, assymmetric, fan-shaped extension to the northwest.

Plate CI 618 was taken mainly for spectrophotometric purposes and will be described in more detail later. The most evident difference between the spectrum of Haro 4 and the spectra of the blue knots associated with NGC 3561 and

IC 1182 is the greater strength of the [O III] λλ4959, 5007 lines relative to [O II] λ3727 in the Haro galaxy.

A high resolution unwidened spectrogram (CI 633, Fig. 5) was taken following the same procedure that was used for the high dispersion plates of NGC 3561 and IC 1182 (i.e. the first-order red and second order ultraviolet regions of the spectrum appearing on the same plate). The λ3729 component of the resolved [O II] λ3727 doublet is substantially stronger than the λ3726 component, suggesting that the electron density is about 200 cm^{-3}. The Hα line is stronger than [N II] λ6583 by a factor of perhaps 20.

Finally, a high resolution widened spectrogram (CI 698, Fig. 6) was obtained, covering the spectral region from 3500 Å to 4550 Å. In addition to [O II] λ3727 and the Balmer series, the emission lines [Ne III] λλ3869, 3968, [O III] λλ4363, 4959, 5007, and He I λ4471 are seen. The lines show no broadening at this dispersion. Because the slit accepted light from the entire east-west extent of the galaxy, an upper limit to the combined internal velocity dispersion and the rotation component of the galaxy about a north-south axis can be set at about 80 km/sec.

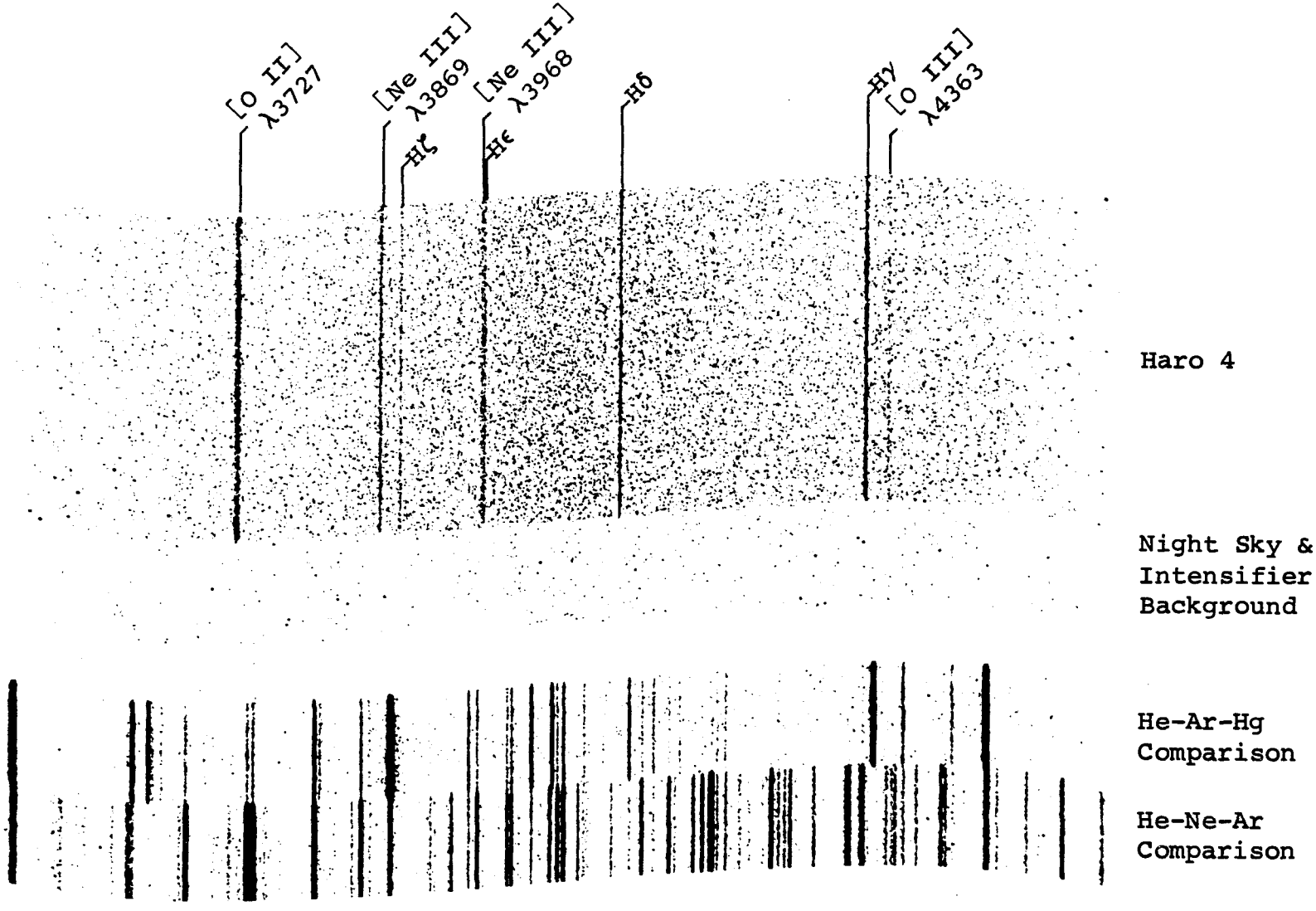

Fig. 6. Widened Spectrogram of Haro 4

Haro 4 has a radial velocity of 582 km/sec. For an assumed Hubble constant of 75 km/sec/Mpc, the distance is 8 Mpc; but this distance is not well-determined, because the peculiar velocity could possibly be of the same order as the observed radial velocity. The dimensions of the bright, symmetrical part of Haro 4 as measured on an 84-inch direct plate are 9.7" by 7.5", and the apparent photographic magnitude given by Markaryan (1967) is 15.5. If the distance is 8 Mpc, then the linear dimensions are 380 pc by 290 pc, and the absolute photographic magnitude is -14.0. It is instructive to compare these values with those for the 30 Doradus nebula in the Large Magellanic Cloud. Shapley and Paraskevopoulos (1937) have estimated that the angular diameter of the nebula is about 25', and Shapley and Wilson (1925) state that the total integrated photographic magnitude of the nebula is not fainter than 4.0. With these values and assuming a distance to the Large Magellanic Cloud of 55 kpc, we obtain for the nebula a diameter of 400 pc and an absolute magnitude of -15.

If, taking an extreme case, we were to suppose that Haro 4 has a peculiar velocity of 1000 km/sec toward us, its distance would be 21 Mpc, giving dimensions of 1000 pc by

800 pc and an absolute magnitude of -16. This assumption, then, would place Haro 4 between 30 Doradus and the knots associated with NGC 3561 and IC 1182 both in physical size and in brightness.

NGC 4163, NGC 4190, and NGC 4485

Short-exposure, unwidened spectrograms at high resolution were taken of these three galaxies. The only galaxy to show a strong emission-line spectrum was NGC 4190. The [O II] λ3727 doublet intensity ratio indicates an average electron density of 200 cm^{-3} or less; Hα is fairly strong, but [N II] λ6583 is not visible.

ASh 6

This system is found in the second list of Ambartsumyan and Shachbazyan (1958) and is described as a blue object near a close pair of galaxies (the 1950 coordinates are right ascension $9^h36^m.5$ and declination $+32^o36'$). One of these galaxies is a spiral, and an 84-inch direct plate shows the blue object to be a series of emission knots in one of the spiral arms. What appeared to be a bright, stellar nucleus of the spiral galaxy was shown by a spectrogram (CI 626) to be a foreground star. The brightest blue knot

has been designated ASh 6 (b), and it has been included in the spectrophotometric program in order that the blue knot NGC 3561 (b) and the blue galaxy Haro 4 might be compared with a bright emission region in a spiral arm. The spectrogram (CI 627) of ASh 6 (b) shows a typical low-excitation emission-line spectrum with lines of [O II], [O III], and the Balmer series being present.

Spectrophotometry

The six plates taken mainly for spectrophotometric purposes are listed in Table 9 along with the relevant data concerning them. The methods used for reducing the plates are described in Appendix II. From the calibration exposure of HD 86986 (for which the spectrophotometric data was supplied by Dr. J. B. Oke) both the transfer characteristic and the spectrophotometric response function of the system were obtained. The calibration of the relative emission line intensities was done empirically from the calibration exposure of an emission knot in the planetary nebula NGC 2392. The relative intensities of the emission lines were corrected for a systematic wavelength effect determined by comparing the relative intensities derived from the NGC 2392

Table 9 Spectrophotometric Plates

All plates were developed for 15 minutes in D-76 at a temperature of 68 °F. Plates CI 615 through CI 618 were developed together. A mechanical tray rocker provided agitation during development.

Plate Number	Object	Filter	Exposure Object	Exposure Sky	Wavelength Range
CI 615*	NGC 2392	$2^m.5$ neutral	30 min	--	3100--7700 Å
CI 616*	HD 86986	$7^m.5$ neutral	30	--	"
CI 617	NGC 3561 (b)	none	112	56 min	"
CI 618	Haro 4	none	24	12	"
CI 627	ASh 6 (b)	none	30	15	"
CI 698	Haro 4	BG 12	90	30	3500--4550

* Calibration plates: the exposure was stepped in ratios 1:2:5:10:20:50.

spectrogram with those found by Minkowski and Aller (1956) for the same part of the nebula.

Table 10 gives the relative emission line strengths, normalized to $H\beta = 100$, for NGC 3561 (b), Haro 4, and ASh 6 (b). It is obvious that there are rather large errors, e.g. the ratios of the intensities of the [O III] lines for NGC 3561 (b) and ASh 6 (b) are in error by about 50 per cent. The relative intensities for Haro 4 (for which a better exposure was obtained) seem to have smaller internal errors, and the Balmer decrement is consistent with radiative recombination. Qualitatively, from the ratio of [O II] λ3727 to the [O III] lines, one can say that NGC 3561 (b) and ASh 6 (b) have lower ionization than Haro 4.

No calibration plates were obtained for the higher dispersion spectrogram (CI 698) of Haro 4. Although the transfer characteristic found from CI 616 may be used with this plate, no system response function for the particular instrumental configuration used is available; therefore, it is possible to compare line intensity ratios only over short wavelength ranges. The particular line intensity ratios of interest are [O II] λ3729/[O II] λ3726 and [O III] λ4363/$H\gamma$. From the former the electron density can be determined, and

Table 10 Relative Emission-Line Intensities

Line		NGC 3561 (b) Plate CI 617	Haro 4 Plate CI 618	ASh 6 (b) Plate CI 627
[O II]	λ3727	232	116	159
[Ne III]	λ3869		42	
Hε [Ne III]	λ3970 λ3968		40	
Hδ	λ4102		35	
Hγ	λ4340		48	64
Hβ	λ4861	100	100	100
[O III]	λ4959	76	144	66
[O III]	λ5007	147	387	122
Hα	λ6563		344	560

from the latter, using the intensity ratio Hγ/[O III] λλ4959, 5007 found from CI 618, the electron temperature is determined. Both of these quantities refer to some kind of average over the region of the galaxy covered by the slit.

Relative line intensities were found from this plate by applying the transfer characteristic curve to the microphotometer tracings of the lines to get intensity profiles and then by comparing total areas under the corrected profiles. The intensity ratio [O III] λ4363/Hγ was found to be 0.215 ± 0.04. From CI 618 the intensity ratio Hγ/[O III] λλ4959,5007 is 0.09.

The equation relating the intensities of the [O III] lines to the physical conditions in the gas (Seaton 1960) is

$$\frac{I(\lambda 4959) + I(\lambda 5007)}{I(\lambda 4363)} = \frac{7.14 \exp (3.30/t)}{1 + 0.038x},$$

where $t = 10^{-4} T_e$

and $x = 10^{-4} N_e t^{-1/2}$.

T_e and N_e are the electron temperature and density, respectively.

Because the dependence on x is weak and x is likely to be a small quantity, we ignore the second term in the denominator of the right-hand side. This simplification will

be seen to be justified by the electron density calculation given below. From the intensity ratios found above,

$$\frac{I(\lambda 4959) + I(\lambda 5007)}{I(\lambda 4363)} = 52$$

and $T_e = 16\ 500\ ^{o}K.$

The error limits on this quantity are estimated to be $\pm 4000\ ^{o}K$.

The [O II] λ3727 doublet was not completely resolved on the microphotometer tracing, but the intensity profile was analyzed into two components having similar profiles and the correct separation for the doublet. The intensity ratio $r = I(\lambda 3729)/I(\lambda 3726)$ is found to be 1.29 ± 0.10. The expression given by Seaton and Osterbrock (1957) for this ratio is

$$r = 1.5\ \frac{1 + 0.33\epsilon + 2.30x(1 + 0.75\epsilon + 0.14\epsilon^2)}{1 + 0.40\epsilon + 9.90x(1 + 0.84\epsilon + 0.17\epsilon^2)},$$

where $\epsilon = \exp(-1.96/t)$

and x and t are defined as before.

Using the electron temperature of 16 500 ^{o}K found above, $t = 1.65$, $x = 7.8 \cdot 10^{-5} N_e$, and $\epsilon = 0.304$. Substituting and reducing, we find $N_e = 217\ cm^{-3}$. The error limits on the ratio r are such that electron densities from less than 100 to about 350 cm^{-3} are possible.

Figure 7 shows spectral-energy distributions for NGC 3561 (b), Haro 4, and ASh 6 (b). For comparison, similar curves are shown for NGC 5253, υ Ori, and a black-body of infinite temperature. The data for NGC 5253 are from photometry by Wood (1966), and those for υ Ori are from photometry by Code (1960). The error bars are estimates of the reliability of each point, based on the uncertainty in the assigned values for the continua of the sky and the object. While one cannot eliminate the possibility that there may be some additional error systematic with respect to wavelength, it is difficult to see how a very large effect of this nature could enter. All of the points for the program objects have been reduced to the rest system. The curves have been normalized so that they are equal at 4590 Å; the slopes are, therefore, somewhat dependent on the accuracy of the points in this wavelength region, and not too much weight should be given to small differences in slope. For example, it is probably not significant that the energy distribution of ASh 6 (b) appears to be slightly steeper than that of a black-body of infinite temperature.

It is clear that although there are small differences in slope, the spectral-energy distributions of the three

Fig. 7. Relative Spectral-Energy Distributions

Each of the curves has been normalized to one scale division at 4590 Å, and the individual graphs have been displaced from each other by the same amount. The three solid-line curves have been included for comparison. The data for NGC 5253 and υ Ori are from photometry by Wood (1966) and Code (1960), respectively. NGC 5253 is a blue irregular galaxy (B-V = 0.44, U-B = -0.19), and υ Ori is a B0 V star.

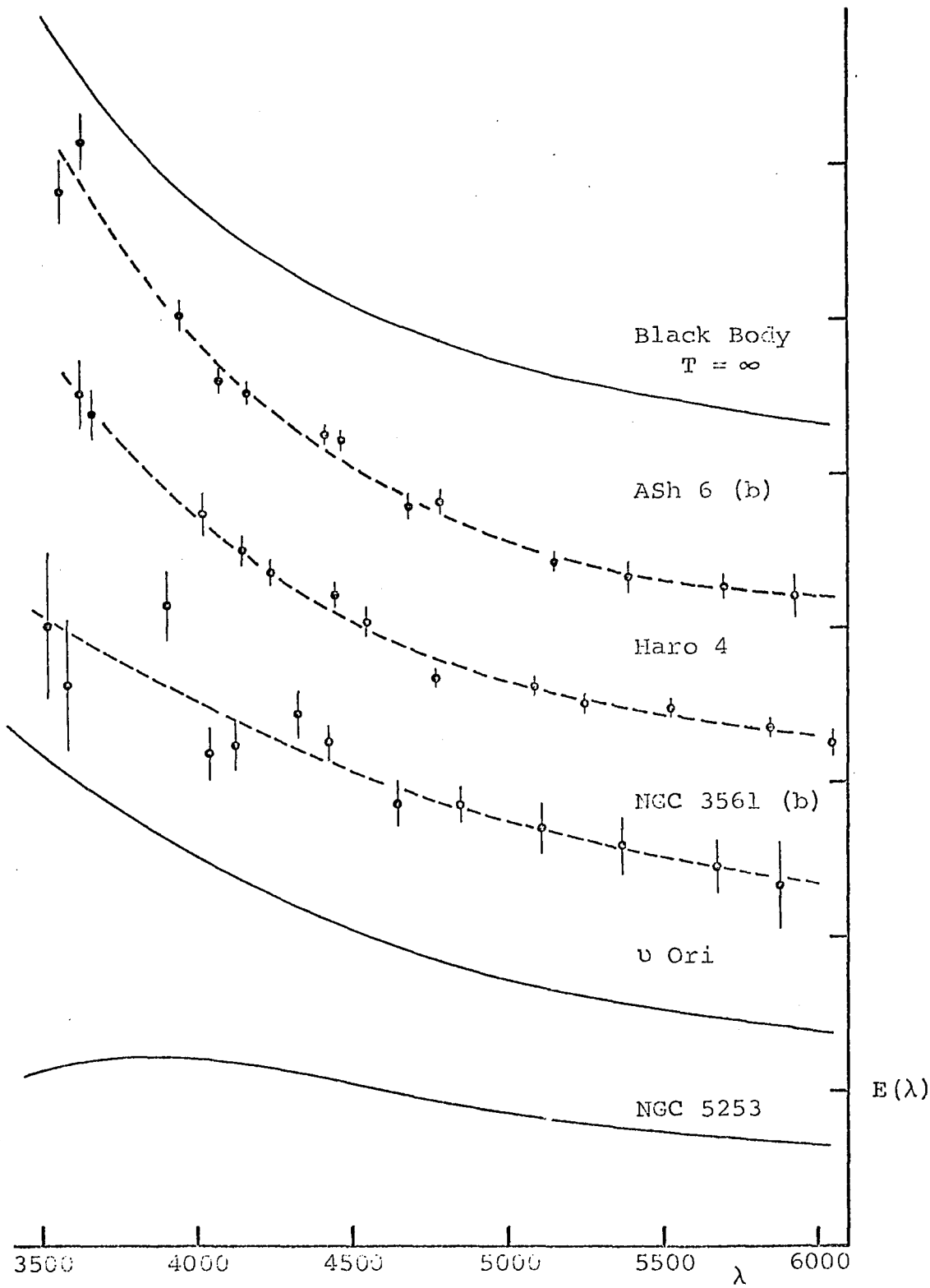

Fig. 7. Relative Spectral-Energy Distributions

objects are qualitatively similar. It is reasonable to suppose that the continuum radiation in the objects originates in each case from the same physical process. Any attempt to explain the continuum radiation must take into account the general absence of detectable absorption lines in the spectra of these objects.

The possibility that the radiation can originate from the synchrotron process seems remote. Known synchrotron sources have $F(\lambda) \sim \lambda^n$, where in general $-2 < n < 0$. For the three program objects, n is in the neighborhood of -4. None of the objects involved in this investigation (with the exception of the blue stellar object near Hydra A) falls near a catalogued radio source.

It is possible to express the continuum radiation of hydrogen (free-bound, free-free, and two-quantum) in terms of the strength of one of the hydrogen lines. The expressions for the emission (in ergs/cm/sec/Hz) in the various continua are (Aller 1956)

$$E(\nu)_{fb} = \frac{N_i N_e K h}{T_e^{3/2}} \exp -\left[\frac{h\nu}{kT_e}\right] \sum_{n_m}^{\infty} \frac{\bar{g}_{n'}}{n'^3} \exp (X_{n'}),$$

$$E(\nu)_{ff} = \frac{N_i N_e k K}{2RT_e^{1/2}} \exp -\left[\frac{h\nu}{kT_e}\right],$$

and $$E(\nu)_{2q} = \frac{N_i N_e K h}{T_e^{3/2}} \sum_{2}^{\infty} \frac{\exp(X_n)}{n^3} \bar{g} E_1(X_n)\ 2X \frac{y\varphi(y)}{3.77},$$

where N_i and N_e are the proton and electron densities,

K is an expression involving constants only,

h is the Planck constant,

T_e is the electron temperature,

k is the Boltzmann constant,

R is the Rydberg constant,

$\bar{g}_n$ and $\bar{g}$ are Gaunt factors for free-bound and free-free transitions, respectively, averaged over the continuum,

n_m is subject to the condition that $n_m^2 > \frac{hR}{\nu}$,

$$X_n = \frac{hR}{n^2 k T_e},$$

$$E_1(X_n) = \int_1^{\infty} \frac{\exp(-rX_n)}{r}\, dr,$$

X is the probability that a recapture to the n = 2 level or any higher level will eventually lead to an atom in the 2s state,

$$y = \frac{\nu}{2.467 \cdot 10^{15}\ \text{Hz}},$$

and $\varphi(y)$ is a function of certain quantum integrals defined by Breit and Teller (1940).

The total continuous emission may, therefore, be written as

$$E(\nu)_c = \frac{N_i N_e K h}{T_e^{3/2}} \left[\sum_2^{\infty} \left(\frac{\exp\ (X_n)}{n^3}\ \bar{g} E_1 (X_n)\ 2X\ \frac{y\varphi(y)}{3.77} \right) \right.$$

$$\left. + \exp\ (-h\nu/kT_e) \left(\frac{kT_e}{2hR} + \sum_{n_m}^{\infty} \frac{\bar{g}_{n'}}{n'^3} \exp\ (X_{n'}) \right) \right].$$

For convenience, we call the quantity in the brackets A; it is a function only of ν and T_e. Aller (1956) has given log A as a function of $1216/\lambda$ for various values of $\theta = 5040/T_e$. The spectral-energy distribution (in wavelength units) of the total continuum emission from hydrogen at T_e = 16 800 ^{o}K is shown in Figure 8.

The energy emitted per cm^3 per sec in a Balmer line is

$$E_{n2} = \frac{N_i N_e K h}{T_e^{3/2}}\ b_n\ \frac{g_{n2}}{8}\ \frac{2R}{n^3} \exp\ (X_n),$$

where b_n is the population deviation factor from the case of thermodynamic equilibrium for the level n.

We may now calculate the equivalent width that one of the Balmer lines would have if the continuum were entirely due to free-bound, free-free, and two-quantum emission

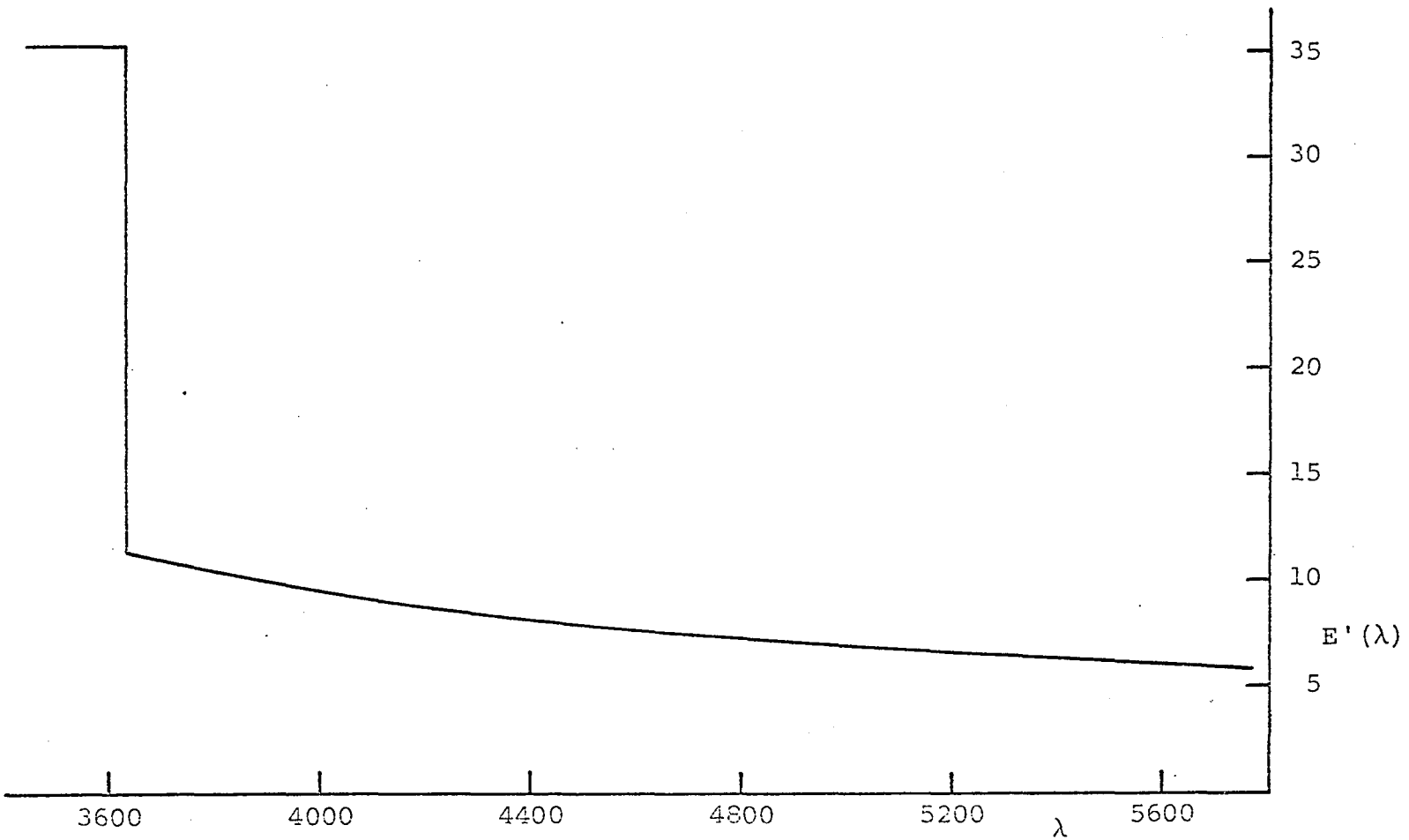

Fig. 8. Hydrogen Emission Continuum

The free-bound, free-free, and two quantum continua have been combined assuming T_e = 16 800°K. The ordinate E'(λ) is proportional to $E(\lambda)/(N_i N_e)$.

from hydrogen. For the Hγ line

$$EW(H\gamma) = \frac{E_{52}}{E(\lambda)_c} = \frac{\lambda^2}{c}\frac{E_{52}}{E(\nu)_c} = \frac{\lambda^2}{c}\frac{2b_5 g_{52} R \exp(X_n)}{2^3 \cdot 5^3 A}$$

$$= 1.26 \cdot 10^{-14}\frac{b_5 g_{52} R \exp(X_n)}{A}.$$

From the graph given by Aller (1956), A was found to be 0.0541 for $\lambda = 4340$ Å and for $T_e = 16\,800\ ^{o}K$. From tabulated values given by Baker and Menzel (1938), $g_{52} = 0.844$ and $b_5 = 0.40$. Case B, for which the gas is optically thick to Lyman radiation, was assumed. Substituting these numbers into the expression given above, we find $EW(H\gamma) = 376$ Å.

The actual equivalent width of Hγ in the spectrum of Haro 4, as measured on plate CI 698, is 7.9 Å. Thus the continuum radiation from the hydrogen gas in the galaxy is completely negligible compared with that from other sources. This result is consistent with the absence of any detectable Balmer discontinuity in the continuum.

It seems most reasonable to suppose that the continuum radiation for NGC 3561 (b), ASh 6 (b), and Haro 4 is coming from stars. If this is the case, virtually all of the radiation in the optical part of the spectrum must come from O and B stars. It is likely that no absorption

features from such a stellar sample would be strong enough to be visible on the spectrograms obtained in this investigation.

IV

GENERAL RESULTS

It is now possible to place the individual observations described in the preceding chapter into a coherent framework within the field of extragalactic studies generally. The four objects that clearly fall outside the domain of this investigation (i.e. the two quasi-stellar objects, the Saakyan star, and the blue object near the Hydra A radio galaxy) are not included in the following discussion.

Summary of Physical Properties of the Blue Condensations

At low dispersion, the emission-line spectra of the blue condensations appear quite similar; it is likely, therefore, that results found for one or two of the condensations may be applied to the others. The best-observed blue condensations in the present program were those associated with NGC 3561 and IC 1182. In both cases the lines were unresolved on high dispersion spectrograms, and it was possible to set an upper limit of about 80 km/sec to the internal velocity dispersion. From the estimated intensity ratios of the components of the [O II] λ3727 doublet, it was

found that the average electron densities ranged from less than 200 cm^{-3} to about 700 cm^{-3}. The electron densities of the fainter condensations were near the lower value.

Burbidge and Burbidge (1962, 1965) have found that the intensity ratio Hα/[N II] λ6583 is typically 3 in the outer regions of spiral galaxies and in irregular galaxies but is usually less than 1 in the nuclear regions of spiral galaxies and in elliptical galaxies. These authors have attributed the differences in relative intensities to differences in excitation conditions. In the present study, this ratio was found to be at least 3 for both NGC 3561 (b) and IC 1182 (e), indicating (unless there are significant differences in chemical abundances) that the excitation conditions in these objects are similar to those found in diffuse nebulae in spiral arms.

The spectral-energy distributions for NGC 3561 (b), Haro 4, and ASh 6 (b) were found to be qualitatively similar and apparently cannot be explained by synchrotron radiation or by free-bound, free-free, or two-quantum emission from hydrogen. The most likely explanation for the continuum radiation in these objects is that it is due to early-type stars.

The Physical Relation of Blue Condensations to Galaxies

The blue knots near NGC 3561, IC 1182, and S 9 are connected by luminous bridges to the elliptical or S0 galaxies with which they are associated; the systems ASh 2 and ASh 3 have no such connections. The spectra of the blue knots for all five systems appear to be qualitatively similar. However, the spectra of the three galaxies in the first group show emission lines, whereas those of ASh 2 and ASh 3 show only K-type absorption spectra. The maximum radial velocity difference between the galaxies and their associated blue condensations for the systems having bridges is 360 km/sec; for ASh 2 and ASh 3 the differences are 800 and 2000 km/sec, respectively.

From these considerations, it seems likely that the blue knots near ASh 2 and ASh 3 are not associated with the elliptical galaxies but are simply blue galaxies (similar to the Haro galaxies) that belong to the same clusters and happen to lie along approximately the same line of sight.

Possible Origins

What can be said about the systems NGC 3561, IC 1182, and S 9, for which there is in each case a definite physical association between the galaxy and the blue

condensation(s)? In Chapter I theories of formation for such systems were divided into three categories: (a) those in which the process is intrinsic to the galaxy (e.g. ejection from the nucleus), (b) those in which the process is governed by external conditions (e.g. condensation from the intergalactic medium), and (c) those in which the process results from an interaction between galaxies (e.g. a tidal effect). For NGC 3561 and IC 1182 there is sufficient photographic and spectroscopic material for a discussion in terms of these categories.

It was proposed in Chapter III that the blue knots and the other peculiarities of IC 1182 could be explained by supposing the gaseous material in the galaxy to be rotationally unstable. Whether or not this explanation is correct, it is unlikely that the large inclination of the emission lines in the galaxy, the string of blue condensations to the east, and the faint, diffuse material on the west side are all unrelated phenomena. In fact, the appearance of strong emission lines in what is morphologically an elliptical or S0 galaxy is suggestive of an intimate involvement of the galaxy in whatever process is taking place.

The blue condensations associated with NGC 3561 apparently cannot be explained in terms of a rotational instability of the gas in the galaxy. Although the sense of rotation of the galaxy (Zwicky and Humason 1961) is such that the side of the galaxy nearest the blue condensations is approaching the observer, the redshifts of the three blue knots increase with increasing distance from the galaxy. The blue condensations and diffuse matter around the spiral component of the system, as well as the large structure extending for about 135 kpc north of the spiral galaxy, indicate that the peculiarities of this system are related to the medium surrounding the galaxies rather than to anything happening within the galaxies themselves. On the other hand, large dust patches seen in elliptical galaxies, such as those found on the south and west sides of NGC 3561 (a), are usually thought to be associated with some sort of internal disruption of the galaxy (e.g. the galaxies identified with the Centaurus A and Fornax A radio sources).

Thus the evidence seems to be contradictory: IC 1182 indicates that the material for the blue condensations in that system most likely came from the gaseous material in the galaxy, whereas the most consistent explanation for

the blue condensations in the NGC 3561 system is condensation from a surrounding gaseous medium. It may be, in spite of the similarities these systems possess, that they represent basicly different phenomena.

It was pointed out in Chapter I that the string of blue condensations south of the elliptical component of NGC 3561 resembles the jet of M 87 in form but has quite different spectroscopic properties. Could the M 87 jet, expanding but not losing its basic form, ever evolve into something having the spectroscopic properties of the blue condensations of NGC 3561? For this to be the case, it is at least necessary that there be associated with the jet a significant mass of non-relativistic plasma. The only evidence that such material may exist in the M 87 jet is the recent detection of X-rays from the vicinity of M 87 (Byram, Chubb, and Friedman 1966; Friedman and Byram 1967), if these X-rays are of thermal origin. At present, it seems more likely that the X-rays represent the high-energy extension of the synchrotron spectrum (Shklovskii 1967; Bradt, Mayer, Naranan, Rappaport, and Spada 1967; Felten 1968), although there are also difficulties with this interpretation (Felten 1968). Of course, the positional accuracy of the X-ray

measurements is not good enough to determine whether the radiation comes from the jet or from some other region of the galaxy.

Thus the hypothesis that the jets in M 87 and NGC 3561 have similar origins must finally be based entirely on their morphological similarity. The jets have no other observed characteristics in common, and even the morphological argument is partially flawed by the large difference in scale of the two phenomena. Although the available observational data do not eliminate the possibility that the two jets are different stages of the same process, they provide very little support for it.

Several similarities have been demonstrated between the blue condensations investigated here and emission nebulae found in the arms of spiral galaxies and in irregular galaxies. The major difference is one of scale: bright emission nebulae with their associated O and B stars typically form systems several tens of parsecs in diameter and have absolute magnitudes of about -11 (although the 30 Doradus nebula is about 400 pc across and has an absolute magnitude of -15). The blue knots associated with NGC 3561 and IC 1182 have characteristic dimensions of 2 to 3 kpc and

absolute magnitudes of -16 to -17. Because diffuse emission nebulae and the blue condensations near NGC 3561, IC 1182, and S 9 both appear to be ionized by hot stars and to have other spectroscopic properties in common, it is difficult to believe that they have resulted from completely unrelated processes.

If it is accepted that both classes of objects have condensed in the recent past from gaseous material of relatively low density (without specifying whether this material has come from the galaxy or from the surrounding medium), then the blue condensations must be counted as recently-formed stellar systems having the dimensions of dwarf galaxies. It cannot be argued that a bright population I component is simply masking a dominent older population, for the linear alignment of the blue condensations associated with both NGC 3561 and IC 1182 implies that the condensations themselves must be young. Such arrangements are unlikely to be stable over a time scale $t \approx (R^3/GM)^{1/2}$, where M is the mass for the main galaxy and R is an average distance from the center of the main galaxy to the blue condensations. For NGC 3561 and IC 1182, t is of the order of 10^8 years.

Suggestions for Future Work

This investigation has necessarily taken the form of a survey. Although much has been learned concerning the physical conditions in the blue knots and the dynamics of the systems to which they belong, no generally satisfactory answer to the question of their origin has been found. There does not seem to be any practical observation that can provide a definite answer to this question. There are, however, a few specific observations that can effectively supplement the present study:

(1) The argument that the gas in IC 1182 is rotationally unstable was based in part on the assumption that the galaxy is actually a flattened system having an inclination to the plane of the sky of about 30°. The rationale for this assumption was that a galaxy having such a large rotational velocity would be likely to be highly flattened. It is, however, not impossible that a galaxy showing a high rotational velocity for the gas might have a nearly spherical stellar distribution, either because the stellar and the gaseous components have different rotational velocities or because the stellar system has not assumed a relaxed configuration. The gaseous component, on the other hand, relaxes

quickly and will, therefore, form a highly flattened system. A direct photograph of the galaxy through an Hα interference filter would give the minor-to-major axis ratio of the projection of the gaseous disc. If the analysis given in Chapter III is correct, this ratio will be found to be about 0.85. If the ratio is substantially less, then the galaxy is being viewed more nearly edge-on than was assumed, and the true rotational velocity is correspondingly less.

(2) Radio observations of the neutral hydrogen in the Hercules and Leo A clusters would be useful. An unusually large amount of neutral hydrogen might indicate that there is a significant mass of intergalactic material in these clusters.

(3) It would be valuable to have a more complete understanding of the NGC 3561 system. Especially useful would be information concerning the dynamics of the blue condensations and diffuse material surrounding and north of the spiral galaxy. The feasibility of studying extremely low surface brightness emission regions at high resolution was demonstrated by the detection of the [O II] λ3727 doublet in the very faint material between the two bright galaxies during the present investigation.

(4) There is a need for a larger sample of systems having one or more blue condensations connected by a luminous bridge. Although such objects are discouragingly infrequent--there is perhaps 1 for every 300 or 400 square degrees--the Sky Survey plates can be searched fairly rapidly for this type of object. Of the systems already known but not yet studied, S 2 and S 42 are probably the most interesting.

APPENDIX I

A SEARCH FOR BLUE KNOTS NEAR ELLIPTICAL GALAXIES

A search for blue objects near elliptical galaxies was made on a blink comparator, using a set of glass copies of the Sky Survey plates at Kitt Peak National Observatory. In general, objects selected were required to have substantially larger or darker images on the O-plate than on the E-plate, to be visible on both plates so as to avoid plate flaws, and to be within a few galaxy diameters of the galaxy with which they are presumed to be associated. Most of the coincidences between galaxies and stellar-appearing blue objects have been ignored for the reasons given in Chapter I.

Approximately 1300 square degrees of sky were examined, including the entire region from 10^h to 14^h right ascension and $+27^\circ$ to $+51^\circ$ declination. More than 100 objects were noted in the original survey; on second examination, many of these proved to be of little interest, and the list given in Table 11 contains 49 systems. Objects from published lists are included if they were also noticed during the present survey.

The first column in Table 11 gives the number assigned to the galaxy in the present survey. The second and third columns give the 1950 epoch coordinates for the galaxy; the fourth and fifth columns give the distance in minutes of arc of the blue knot from the center of the galaxy, north and east being regarded as positive directions. In some cases more than one blue knot was found near a single galaxy. If there is a visible bridge connecting the blue knot to the galaxy, this fact is indicated by an X in column six; a question mark indicates a possible bridge. Column seven gives general remarks and other designations for the galaxies. The designations Arp, VV, and ASh refer, respectively, to the Atlas of Peculiar Galaxies (Arp 1966), the Atlas and Catalogue of Interacting Galaxies (Vorontsov-Velyaminov 1959), and the anonymous galaxies in the list by Ambartsumyan and Shachbazyan (1957).

Table 11 Blue Knots Near Elliptical Galaxies

S	α 1950	δ	$\Delta\alpha$	$\Delta\delta$	Bridge	Remarks
1	$01^h47^m.3$	$+35^\circ59'$	+0.1	+0.1		
2	01 53.5	+36 32	+0.5	-0.1	X	
3	04 09.7	-03 10	-0.8	-0.5		
4	09 46.8	+37 47	-0.2	+0.2		Stellar image
5	09 53.2	+37 49	-0.8	-1.6		Stellar image
6	09 55.7	+39 52	-0.1	-0.3		
			+0.0	-0.7		
7	10 02.5	+29 19	-0.6	+0.3		
8	10 04.4	+34 41	+0.6	+0.0	X	
9	10 04.4	+38 07	+0.3	+0.0	X	
10	10 05.8	+30 08	-0.2	+0.2		
11	10 13.6	+36 00	-0.3	+1.2		Stellar image
12	10 16.1	+38 37	-0.6	+0.8		
			-0.8	+1.0		
13	10 22.6	+37 37	-0.3	+0.0		
14	10 33.4	+30 05	+0.0	-0.2		
15	10 35.9	+28 55	+0.5	-0.3		
16	10 43.1	+29 31	-1.0	-0.5		Stellar image
17	10 45.0	+39 12	+0.6	+0.6	?	Stellar image
18	10 49.9	+28 49	+0.3	-0.4		Stellar image
19	10 53.3	+44 42	+0.0	+0.2		
			-0.5	+0.3		

Table 11 Continued

S	α 1950	δ	Δα	Δδ	Bridge	Remarks
20	$10^h58^m.3$	+28°29'	-0!1	+0!1		
21	11 02.3	+47 15	+0.0	-0.2		
22	11 02.7	+30 25	+1.1	+0.0		Stellar image
23	11 03.0	+34 03	+0.5	+0.2		
24	11 08.0	+28 35	+0.0	+0.8		ASh 2
			-0.2	+0.3		Stellar image
			+0.1	+1.0		Stellar image
25	11 08.5	+28 58	+0.0	-0.5	X	NGC 3561, Arp 105, VV 237
			-1.1	-0.1		Stellar image
26	11 08.9	+03 34	-0.4	-0.1		
27	11 13.9	+29 31	+0.3	-0.1		ASh 3
28	11 16.0	+42 29	+0.3	-0.1		
29	11 16.8	+29 27	-0.2	-0.6		
30	11 28.6	+06 26	-0.1	-0.8		
31	11 30.6	+38 40	+0.0	+0.1		
32	11 38.5	+31 23	+0.9	+0.7		
33	11 48.5	+28 29	-0.4	-0.7		Stellar image
34	11 52.7	+37 10	+0.1	-0.3	X	
35	11 58.8	+34 33	-0.2	-0.1		
36	11 59.8	+27 48	+0.1	-0.1		
37	12 43.8	+36 20	+0.5	-0.9	?	Stellar image

Table 11 Continued

S	α 1950	δ	Δα	Δδ	Bridge	Remarks
38	$12^h49^m.6$	$+27^\circ45'$	+0!4	-0!7		Stellar image
39	13 09.0	+39 35	-0.2	-0.4		
40	13 09.2	+31 47	-0.8	-0.1		
41	13 12.2	+26 24	-0.6	-2.3	X	Arp 196
42	13 12.7	+26 51	-0.2	-0.1	?	Stellar image
			-0.9	-0.6		Stellar image
43	13 14.0	+37 15	-0.6	-0.1	?	
44	13 14.0	+31 38	+0.1	+0.1		
45	13 31.0	+37 20	+0.3	+0.0		
46	13 32.5	+34 08	-0.5	+0.9		
47	13 37.8	+27 21	-0.1	-0.9		
48	13 55.1	+29 02	+0.1	-0.2		
49	14 02.7	+42 01	+0.0	+0.3		

APPENDIX II

THE CALIBRATION OF IMAGE-TUBE SPECTROGRAMS

When an image tube has sufficiently high gain and the scintillation brightness distribution and the transfer camera optics meet certain conditions, virtually all of the scintillations produced at the phosphor can be recorded on a photographic plate. Such a system has a response characteristic that is rather different from that of a photographic plate alone. The nature of this difference can best be understood by considering a simplified model of the process.

Suppose that the scintillations recorded on the plate each produce blackened regions of area s having a transmittance τ. If these scintillations are recorded at a rate r cm^{-2} sec^{-1} and if the superimposed scintillations combine in a linear manner, the change in transmittance for a large region on the plate in a time interval dt is given by

$$dT = -Ts\tau r\, dt.$$

Integrating,

$$\ln T = -s\tau rt$$

where t is the total exposure time. The density is

$$D = -\log T = -\log e^{-s\tau rt} = s\tau rt \log e.$$

With a range of sizes and densities for the recorded scintillations, the partial densities found for each small interval in scintillation size and density can be simply added together; as a result, the plate density remains linear with exposure.

For an electronographic system, in which the photoelectrons directly expose an electron-sensitive emulsion, this linear relation holds over an extremely wide density range (Walker and Kron 1967). The range of validity is restricted for the TSE intensifier used in this study, principally by non-linear photographic effects entering when scintillations are combined. When one scintillation exposes a part of the plate that has been exposed by a previous scintillation, the resulting density is not, in general, the sum of the densities the individual scintillations would have had if they had occurred alone. For scintillations bright enough to be singly recorded, the density resulting from an overlap is less than the sum of the individual densities; the graph of density against exposure, therefore, begins to turn down at a density at which overlaps begin to

be important. Furthermore, if there are any scintillations too weak to be recorded directly, these may, nevertheless, produce sublatent images, which become developable when the same part of the plate is exposed by other scintillations. This effect, if present, will be seen as a "toe" on the lower part of the density-exposure curve. A typical example of this curve is shown in Figure 9; the turnover at high densities and a very slight toe at low densities are both visible. Because this curve is to some extent independent of non-linear photographic effects, especially for the region between densities of 0.1 and 1.0, the calibration procedure is much less sensitive to small variations in development conditions between plates than is that for conventional photographic spectrophotometry. Thus it is possible to make quantitative comparisons between plates developed under similar, but not necessarily identical, conditions.

The Calibration of the Continuum

The actual calibration procedure is similar to that used for conventional photographic spectrophotometry, but there are some special problems. It is necessary to have a spectrophotometric standard that is sufficiently faint that good calibration spectrograms may be obtained. For the

Fig. 9. Transfer Characteristic Curve for Image-Tube Camera

specific equipment used in this study, a standard star of about 15th magnitude is required. Because no suitable standards exist at this magnitude, it was necessary to use a star of magnitude 7.9 (HD 86986) and a 7.5 magnitude Inconel-on-quartz attenuating filter, which is closely neutral over the relevant spectral range. Spectrophotometric data for HD 86986 were kindly supplied by Dr. J. B. Oke.

During the exposure of the calibration plate, the plate drive rate was changed in such a way as to obtain six spectra with relative exposures 1, 2, 5, 10, 20, and 50. A microphotometer tracing across such a spectrogram at any fixed wavelength gives six density values corresponding to the known relative exposures. At each wavelength for which such a tracing is made, an independent graph of density against relative exposure results. If there are no gross differences in the character (e.g. focus) of the scintillations recorded in different regions of the spectrogram, these curves will be the same except for uniform expansions or contractions of the relative-exposure scale. Thus, by multiplying each set of exposure values by a constant, it is possible to place the density values on a single smooth curve. This curve (Fig. 9) gives the transfer

characteristic of the combination of the image tube and the photographic plate. The set of constants (one for each wavelength at which a tracing was made) by which the exposure values were multiplied are in direct proportion to the exposures at the various wavelengths. In other words, if at 5000 Å in the stellar spectrum the photographic plate receives half the light from the phosphor that it does at 4000 Å, the relative exposure values will have to be multiplied by constants in the ratio of 1:2 in order to bring the two density vs. relative exposure curves into alignment. Because the relative spectral-energy distribution of the star is known, a relative response function for the entire system can be found; this is illustrated in Figure 10.

This response function has been corrected for the effect of the 7.5 magnitude attenuating filter; the spectral transmission of this filter was taken into account by assuming that its density at any wavelength was proportional to the density (at the same wavelength) of a similar filter having an attenuation of 2.5 magnitudes. The spectral transmission of this latter filter was measured on a spectrophotometer.

Fig. 10. Relative System Response Function

This system response function, which has been normalized to the peak response, was obtained with a 300 line/mm grating blazed at 4000 Å in the first order. The spectral region near 5000 Å was centered on the image-tube phosphor.

The microphotometer tracings of the galaxy spectrograms were obtained in the same manner as those of the standard star spectrogram, i.e. the spectrograms were traced in the direction perpendicular to the dispersion at certain selected wavelengths. The microphotometer slit length in all cases corresponded to about 100 Å on the photographic plate. Densities were obtained both for the object plus sky and for the sky alone. With the aid of the transfer characteristic curve, these densities were transformed into relative exposure values. Subtracting the sky exposure values from the object plus sky exposure values gives the relative flux at the photographic plate from the object alone; dividing these numbers by the system response for each respective wavelength gives the relative spectral-energy distribution for the object.

The Calibration of the Emission Lines

The calibration of the emission spectrum presents special problems because the central density for some of the emission lines goes beyond the range of densities for which the transfer characteristic curve can be accurately determined. Even for the weaker lines there are advantages to calibrating the emission lines separately from the continuum.

Accordingly, a calibration spectrogram was taken of a condensation immediately south of the central star in the planetary nebula NGC 2392. This spectrogram was obtained in the same manner as that of the standard star HD 86986, i.e. the plate trail rate was changed to give a set of exposures having known ratios. Each emission line was used to derive the line growth as a function of exposure. If T is the transmission of some part of the spectrogram and T_o is the transmission for clear plate, we shall refer to the quantity $(1 - T/T_o)$ as the deflection. The deflection at the line center was used as a measure of line strength, and the plot of this parameter as a function of exposure (in arbitrary units) is shown in Figure 11. This curve results from combining data for many different lines.

For objects having a strong continuum, a certain amount of care must be exercised in removing the effect of the continuum from the deflection for the line. When the central density of the line lies on the linear part of the transfer characteristic curve, i.e. for central densities greater than 0.1 and less than 1.0, the deflection the line would produce in the absence of a continuum is $(1 - T/T_c)$, where T is the measured transmission at the line center and

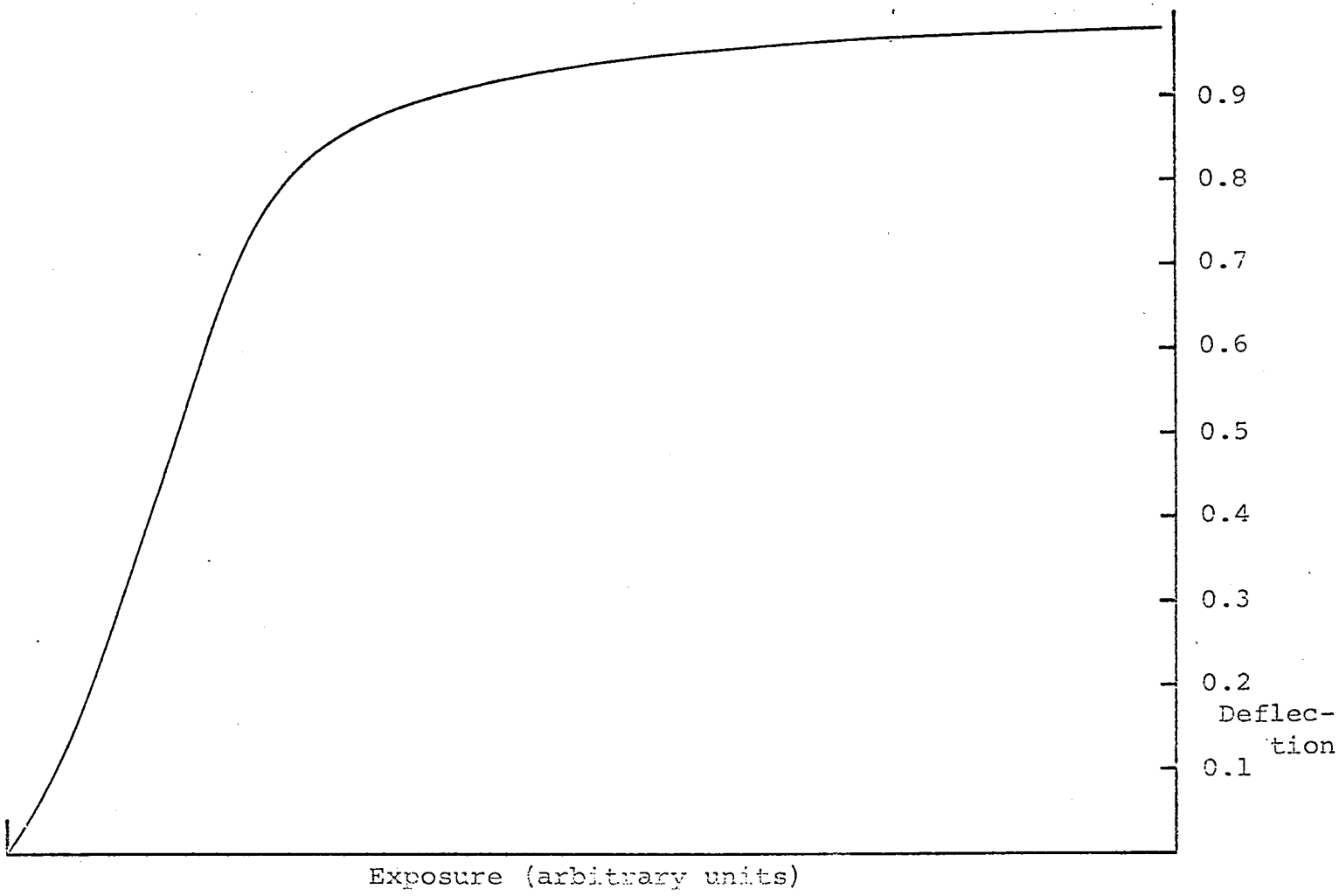

Fig. 11. Calibration Curve for Emission Lines

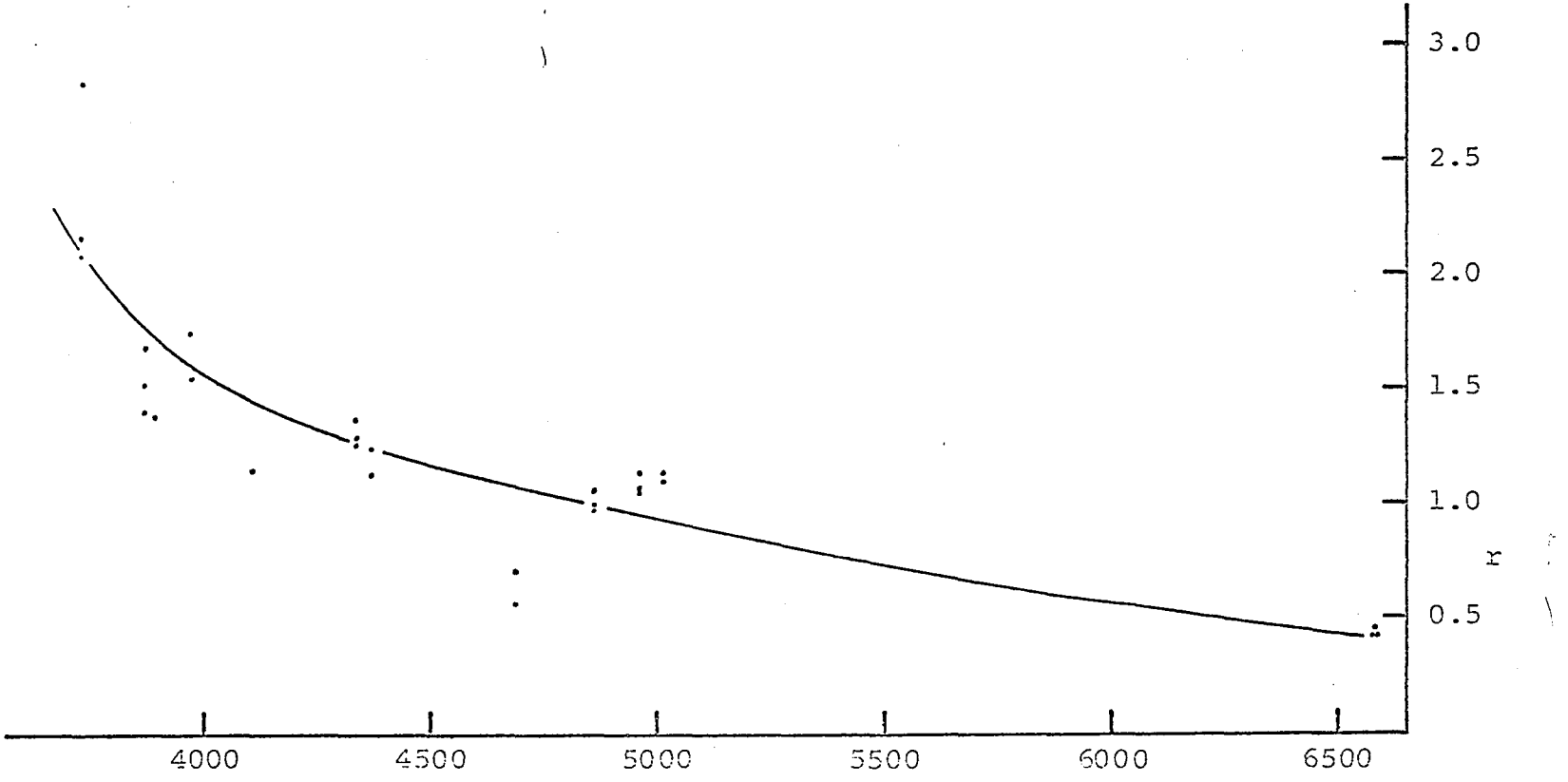

Fig. 12. Systematic Error in Emission Line Intensities

The ordinate r is the ratio of the line intensities found in the present study to those found by Minkowski and Aller (1956).

T_c is the transmission for the nearby continuum. For lines that have central densities outside of this range, it is necessary to correct for the nonlinear combination of continuum and line densities; this correction can be made if the approximate slope of the transfer characteristic curve at the density of the line center is known.

In principle, the system response function found from the continuum standard can now be used to derive relative line intensities. The calibration of the emission lines can, however, be quite sensitive to systematic spectrograph focus effects. That there is indeed a systematic error in the line intensities is shown in Figure 12, which gives the ratios of the line intensities determined by the present techniques to those found by Minkowski and Aller (1956) for the same region in NGC 2392. The line intensities quoted in this investigation have been corrected for this systematic effect.

REFERENCES

Aller, L. H. 1956, Gaseous Nebulae (London: Chapman and Hall, Ltd.).

Ambartsumyan, V. A. 1958, la Structure et l'Evolution de l'Univers (Brussels: R. Stoops), p. 241.

_____. 1961, A. J., 66, 536.

_____. 1962, Trans. I. A. U., XI B, 145.

_____. 1965, The Structure and Evolution of Galaxies (New York: Interscience Publishers), p. 1.

Ambartsumyan, V. A., and Shachbazyan, R. K. 1957, Doklady Akad. Nauk Armyanskoy S. S. R., 25, 185.

_____. 1958, Doklady Akad. Nauk Armyanskoy S. S. R., 26, 277.

Arp, H. 1966, Atlas of Peculiar Galaxies (Pasedena: California Institute of Technology).

Baade, W. 1956, Ap. J., 123, 550.

Baade, W., and Minkowski, R. 1954, Ap. J., 119, 215.

Baker, J. G., and Menzel, D. H. 1938, Ap. J., 88, 52.

Baum, W. A. 1967, Science, 154, 112.

Braccesi, A., Lynds, C. R., and Sandage, A. 1968, Ap. J. (Letters), 152, L105.

Bradt, H., Mayer, W., Naranan, S., Rappaport, S., and Spada, G. 1967, Ap. J. (Letters), 150, L199.

Breit, G., and Teller, E. 1940, Ap. J., 91, 215.

Burbidge, E. M., and Burbidge, G. R. 1959, Ap. J., 130, 629.

Burbidge, E. M., and Burbidge, G. R. 1961, A. J., 66, 541.

_____. 1962, Ap. J., 135, 694.

_____. 1965, Ap. J., 142, 634.

Burbidge, E. M., Burbidge, G. R., and Hoyle, F. 1963, Ap. J., 138, 873.

Byram, E. T., Chubb, T. A., and Friedman, H. 1966, Science, 152, 66.

Code, A. D. 1960, in Stellar Atmospheres, ed. Jesse L. Greenstein (Chicago: University of Chicago Press), p. 83.

DuPuy, D. L. 1967, unpublished M. A. thesis, Wesleyan University.

_____. 1968, Pub. A. S. P., 80, in press.

Felten, J. E. 1968, Ap. J., 151, 861.

Friedman, H., and Byram, E. T. 1967, Science, 158, 257.

Haro, G. 1956, Bol. Obs. Ton. y Tac., No. 14, 8.

Hiltner, W. A. 1959, Ap. J., 130, 340.

Hiltner, W. A., and Iriarte, B. 1958, Ap. J., 128, 443.

Humason, M. L., Mayall, N. U., and Sandage, A. R. 1956, A. J., 61, 97.

Kinman, T. D. 1965, Ap. J., 142, 1241.

Lutnes, J. H., and Davidson, D. 1966, Pub. A. S. P., 78, 551.

Lynds, C. R., and Villere, G. 1965, Ap. J., 142, 1296.

Markaryan, B. E. 1967, Astrofizika, 3, 54.

Minkowski, R. 1961, in Proceedings of the Fourth Berkeley Symposium on Mathematical Statistics and Probability, ed. Jerzy Neyman (Berkeley: University of California Press), III, p. 245.

Minkowski, R., and Aller, L. H. 1956, Ap. J., 124, 93.

Morgan, W. W. 1959, Pub. A. S. P., 71, 92.

Oort, J. H. 1958, in Stellar Populations, ed. D. J. K. O'Connell, S. J. (Amsterdam: North Holland Publishing Co.), p. 415.

Saakyan, K. A. 1965, Astrofizika, 1, 126, (English trans. Astrophysics, 1, 78).

Sandage, A. 1966, Ap. J., 145, 1.

Sandage, A., and Luyten, W. J. 1967, Ap. J., 148, 767.

Schmidt, M. 1965, Ap. J., 141, 1.

Seaton, M. J. 1960, Repts. Prog. in Phys., 23, 313.

Seaton, M. J., and Osterbrock, D. E. 1957, Ap. J., 125, 66.

Shachbazyan, R. K., and Iskudaryan, S. T. 1959, Doklady Akad. Nauk Armyanskoy S. S. R., 28, 53.

Shapley, H., and Paraskevopoulos, J. S. 1937, Ap. J., 86, 340.

Shapley, H., and Wilson, H. H. 1925, Harvard Circular 271.

Shklovskii, I. S. 1955, Astr. Zh., 32, 215.

_____. 1967, Astr. Zh., 44, 58, (English trans. Soviet Astr.--AJ, 11, 45.

Stockton, A. N. 1968, A. J., 73, in press.

Tifft, W. G. 1963, A. J., 68, 302.

Vorontsov-Velyaminov, B. A. 1959, Atlas and Catalogue of Interacting Galaxies (Moscow: Moscow State University).

Walker, M. F., and Kron, G. E. 1967, Pub. A. S. P., 79, 551.

Wood, D. B. 1966, Ap. J., 145, 36.

Zwicky, F. 1956, Ergebnisse der Exakten Naturwissenschaften, 29, 344.

_____. 1958, l'Astronomie, 72, 285.

_____. 1967a, Adv. in Astr. and Ap. (New York: Academic Press), 5, 267.

_____. 1967b, Astrofizica, 3, 525.

_____. 1967c, Pub. A. S. P., 79, 444.

Zwicky, F., and Humason, M. L. 1961, Ap. J., 133, 794.